

**UNIVERSITY OF TURKISH AERONAUTICAL ASSOCIATION
INSTITUTE OF SCIENCE AND TECHNOLOGY**

**PERFORMANCE ANALYSIS OF REPAIRED CARBON FIBER COMPOSITE
MATERIALS WHICH HAVE BEEN MANUFACTURED IN AEROSPACE
INDUSTRY**



MASTER THESIS

Fikret Cem SÖNMEZ

Institute of Science and Technology

Mechanical and Aeronautical Engineering

SEPTEMBER, 2016

**UNIVERSITY OF TURKISH AERONAUTICAL ASSOCIATION
INSTITUTE OF SCIENCE AND TECHNOLOGY**

**PERFORMANCE ANALYSIS OF REPAIRED CARBON FIBER COMPOSITE
MATERIALS WHICH HAVE BEEN MANUFACTURED IN AEROSPACE
INDUSTRY**

MASTER THESIS

Fikret Cem SÖNMEZ

1303720007


Institute of Science and Technology

Mechanical and Aeronautical Engineering

Thesis Supervisor: Assoc. Prof. Dr. Murat DEMİRAL

Türk Hava Kurumu Üniversitesi Fen Bilimleri Enstitüsü'nün 1303720007 numaralı Yüksek Lisans öğrencisi "Fikret Cem Sönmez " ilgili yönetmeliklerin belirlediği gerekli tüm şartları yerine getirdikten sonra hazırladığı "HAVACILIKTA KULLANILMAKTA OLAN KARBON FİBER KOMPOZİT MALZEMELERİN ONARIM SONRASI PERFORMANSLARININ ANALİZİ" başlıklı tezini, aşağıda imzaları bulunan jüri önünde başarı ile sunmuştur.

Tez Danışmanı : Doç. Dr. Murat DEMİRAL
Türk Hava Kurumu Üniversitesi



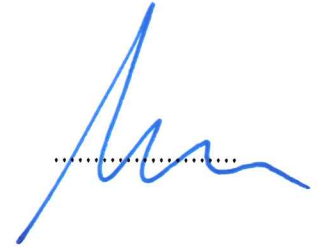
Jüri Üyeleri : Doç. Dr. Murat DEMİRAL
Türk Hava Kurumu Üniversitesi



: Yrd. Doç. Dr. Munir Ali ELFARRA
Yıldırım Beyazıt Üniversitesi



: Yrd. Doç. Dr. Mustafa KAYA
Yıldırım Beyazıt Üniversitesi



Tez Savunma Tarihi: 07.09.2016

**UNIVERSITY OF TURKISH AEROSPACE ASSOCIATION
INSTITUTE OF SCIENCE AND TECHNOLOGY**

Submitted by Fikret Cem SÖNMEZ in partial fulfillment of the requirements for degree of Master of Science in Mechanical and Aeronautical Engineering. “PERFORMANCE ANALYSIS OF REPAIRED CARBON FIBER COMPOSITE MATERIALS WHICH HAVE BEEN MANUFACTURED IN AEROSPACE INDUSTRY” I hereby declare that all information in this document has been obtained and presented in accordance with academic rules and ethical conduct. I also declare that, as required by these rules and conduct, I have fully cited and referenced all material and results that are not original to this work.

01.09.2016

Fikret Cem SÖNMEZ



ACKNOWLEDGEMENTS

My ambition to obtain a master degree was fulfilled mainly because of the support and guidance I received from my former advisor Doç. Dr. Ferhat Kadiođlu. He has helped me at various stages during my studies and this includes providing me with a well defined thesis problem, equipping me with the necessary tools and techniques for achieving my objectives, and willingly sharing his knowledge and ideas with me. His active participation at every facet of my research work and mentoring has shaped my overall research outlook. I am extremely grateful to him for being my adviser during his stay at University of Turkish Aeronautical Association.

I would like to express my sincere gratitude to Doç. Dr. Murat Demiral for his sound advice and constructive criticisms in the evaluation of the experimental results. He has helped me at the final stage of my thesis and willingly sharing his knowledge and ideas with me.

I would like to special thanks to my all Pınar Sönmez and my dear daughter Ayşe Duru Sönmez for their loves and encouragement.

I would like to express my deep gratitude to my family Ayşe Hilal Sönmez, Enis Sönmez, Yiđit Can Sönmez, Fikret Özbek, Süheyla Özbek and İlgin Özdabađ for their trust and encouragement.

I would like to express my deepest gratitude to Arif Murat Tamaç and Alper Serkan Erdemli for their trust and encouragement.

I would like to special thanks to Irmak Polat for her helps and suggestions.

I would like to express deep gratitude to Prof. Dr. Zekiye Suludere for her helps.

I would like to express deep gratitude to my colleagues Mert Ergün, Erdem Çolak, Alper Madenođlu, Ahmet Erdođan, Tolga Tolon, Umut Caglak, Yavuz Akalın, Erdem İlhan for their help to complete my study.

I would like to thank to my friends Ender Şaşal, Haşim Can, Hasan Püskül and Enes Erol for their friendship and being my fellow on my master study.

To my grandfather İsmail Fikret ÇELENLİGİL

Remember with love and longing...

September 2016

Fikret Cem SÖNMEZ

TABLE OF CONTENT

ACKNOWLEDGEMENTS	iv
TABLE OF CONTENT	v
LIST OF TABLES	vii
LIST OF FIGURES	viii
ABBREVIATIONS	x
ABSTRACT	xi
ÖZET.....	xiii
CHAPTER ONE	1
1. INTRODUCTION	1
CHAPTER TWO	5
2. COMPOSITE MATERIALS	5
2.1 Compare of Advantages of Composite Materials and Metallic Parts	8
2.2 Compare of Disadvantages of Composite Materials and Metallic Parts	8
2.3 General Advantages of Composite Materials.....	9
2.4 Carbon Fiber.....	9
CHAPTER THREE	10
3. REPAIR OF COMPOSITE MATERIALS	10
3.1 Scarf Repair.....	12
CHAPTER FOUR	16
4. TEST METHODS	16
4.1 Nondestructive Inspection.....	16
4.1.1 Through Transmission Inspection	17
4.2 Destructive Inspection.....	18
4.2.1 Tensile Test	18
CHAPTER FIVE	20
5. EXPERIMENTAL DATA	20
5.1 Test Specimens.....	20
5.1.1 Ply Orientation of the 0-90-Degree Test Specimens.....	20
5.1.2 Ply Orientation of the 15-Degree Test Specimens	21
5.1.3 Ply Orientation of the 30-Degree Test Specimens	21
5.1.4 Ply Orientation of the 45-Degree Test Specimens	21
5.1.5 Ply Orientation of the 60-Degree Test Specimens	22
5.2 Manufacturing Data for the Test Specimens.....	22
5.2.1 Autoclave Report.....	24
CHAPTER SIX	26
6. RESULT & ANALYSIS	26
6.1 Tensile Test Results for the Repaired Test Specimens	26
6.1.1 Tensile Test Results for the 0°-90° Test Specimens	26
6.1.2 The Tensile Test Results for the 15° Test Specimens	31
6.1.3 The Tensile Test Results for the 30° Test Specimens	35
6.1.4 The Tensile Test Results for the 45° Test Specimens	39

6.1.5 The Tensile Test Results for the 60° Test Specimens	43
6.2 Summary of Chapter	47
CHAPTER SEVEN	52
7. CONCLUSIONS	52
7.1 Recommended Future Research	53
REFERENCES	54
RESUME	57



LIST OF TABLES

Table 5.1	: Ply orientation of the 0°-90° test specimens.....	20
Table 5.2	: Ply orientation of the 15° test specimens.....	21
Table 5.3	: Ply orientation of the 30° test specimens.....	21
Table 5.4	: Ply orientation of the 45° test specimens.....	22
Table 5.5	: Ply orientation of the 60° test specimens.....	22
Table 6.1	: The tensile test results for the 0°-90° test specimens.	27
Table 6.2	: The tensile test results of the 15° test specimens.....	31
Table 6.3	: The tensile test results of the 30° test specimens.....	35
Table 6.4	: The tensile test results of the 45° test specimens.....	40
Table 6.5	: The tensile test results of the 60° test specimens.....	44
Table 6.6	: The tensile test results of the unrepaired test specimens.	47
Table 6.7	: The tensile test results of the repaired test specimens.	49
Table 7.1	: Average ultimate strength points for all of the test specimens.	52
Table 7.2	: Average yield strength points for all of the test specimens.	53

LIST OF FIGURES

Figure 1.1	: Composite materials.....	1
Figure 1.2	: Composite materials.....	2
Figure 1.3	: Impact damage example 1.....	3
Figure 1.4	: Impact damage example 2.....	3
Figure 1.5	: Damage types on composite structures	4
Figure 2.1	: General reinforcement types.	5
Figure 2.2	: Compare of a human hair and carbon-fiber.	6
Figure 2.3	: Random fiber composites.....	6
Figure 2.4	: Continuous fiber composites.....	7
Figure 2.5	: Particulate composites.....	7
Figure 2.6	: Flake composites.....	7
Figure 2.7	: Filler composites.	8
Figure 3.1	: Main types of joint configuration used for repairs to composite structure.	11
Figure 3.2	: Repair types and repetitiveness table.	12
Figure 3.3	: Scarf repair.	13
Figure 3.4	: NDI method - tap inspection.	14
Figure 3.5	: Taper remove of laminates.....	14
Figure 3.6	: Scarf Repair taper laminate removal example 1.	15
Figure 3.7	: Scarf Repair taper laminate removal example 2.	15
Figure 4.1	: Ultrasonic inspection.....	16
Figure 4.2	: NDI method – TTU inspection.....	17
Figure 4.3	: NDI method – manual TTU inspection.....	17
Figure 4.4	: Universal tensile test machine.....	18
Figure 4.5	: Tensile test.....	19
Figure 5.1	: Ply sequence of the test specimens.	23
Figure 5.2	: Test Specimens.....	24
Figure 5.3	: Pressure/Temperature diagram.....	25
Figure 6.1	: Four pieces from the 0°-90° test specimens in the tensile stress/tensile strain graph.	26
Figure 6.2	: The unrepaired 0°-90° test specimens after the tensile test.....	27
Figure 6.3	: The repaired 0°-90° test specimens after the tensile test.....	28
Figure 6.4	: The repair plies of the 0°-90° test specimens.....	29
Figure 6.5	: The yield strength points of the 0°-90° test specimens.	29
Figure 6.6	: The SEM view 1.1 for the 0°-90° test specimens.	30
Figure 6.7	: The SEM view 1.2 for the 0°-90° test specimens.	30
Figure 6.8	: Four pieces from the 15° test specimens in the tensile stress/tensile strain graph.	31
Figure 6.9	: The unrepaired 15° test specimens after the tensile test.	32
Figure 6.10	: The repaired 15° test specimens after the tensile test.	33

Figure 6.11 :	The breakage angle on the 15° test specimens after the tensile test.	33
Figure 6.12 :	The SEM micrograph 2.1 for the 15° test specimens.....	34
Figure 6.13 :	The SEM micrograph 2.2 for the 15° test specimens.....	34
Figure 6.14 :	Four pieces from the 30° test specimens in the tensile stress/tensile strain graph.	35
Figure 6.15 :	The unrepaired 30° test specimens after the tensile test	36
Figure 6.16 :	The breakage points of the repaired 30° test specimens.	37
Figure 6.17 :	The repaired 30° test specimens after the tensile test.	37
Figure 6.18 :	The yield strength points of the 30° test specimens.	38
Figure 6.19 :	The SEM micrograph 3.1 for the 30° test specimens.....	38
Figure 6.20 :	The SEM micrograph 3.2 for the 30° test specimens.....	38
Figure 6.21 :	The SEM micrograph 3.3 for the 30° test specimens.....	39
Figure 6.22 :	Four pieces from the 45° test specimens in the tensile stress/tensile strain graph.	39
Figure 6.23 :	The unrepaired 45° test specimens after the tensile test.	40
Figure 6.24 :	The repaired 45° test specimens after the tensile test.	41
Figure 6.25 :	The repaired 45° test specimens after the tensile test.	42
Figure 6.26 :	The SEM micrograph 4.1 for the 45° test specimens.....	42
Figure 6.27 :	The SEM micrograph 4.2 for the 45° test specimens.....	42
Figure 6.28 :	The SEM micrograph 4.3 for the 45° test specimens.....	43
Figure 6.29 :	Four pieces from the 60° test specimens in the tensile stress/tensile strain graph.	43
Figure 6.30 :	The unrepaired 60° test specimens after the tensile test.	44
Figure 6.31 :	The repaired 60° test specimens after the tensile test.	45
Figure 6.32 :	The SEM micrograph 4.1 for the 60° test specimens.....	46
Figure 6.33 :	The SEM micrograph 4.2 for the 60° test specimens.....	46
Figure 6.34 :	The maximum tensile stress resistances for all of the unrepaired test specimens compared in the same graph.	48
Figure 6.35 :	The maximum tensile stress resistances for all of the repaired test specimens compared in the same graph.....	48
Figure 6.36 :	Average ultimate strength points of the unrepaired test specimens.	50
Figure 6.37 :	Average ultimate strength points of the repaired test specimens.	50
Figure 6.38 :	The tensile stress/tensile strain diagram for the unrepaired test specimens.	51
Figure 6.39 :	The tensile stress/tensile strain diagram for the repaired test specimens.	51

ABBREVIATIONS

UD	:	Unidirectional
SEM	:	Scanning Electron Microscope
NDI	:	Nondestructive Inspection
NDE	:	Nondestructive Examination
NDT	:	Nondestructive Test
RVI	:	Remote Visual Inspection
TTU	:	Through Transmission Inspection
UTS	:	Ultimate Strength

ABSTRACT

PERFORMANCE ANALYSIS OF REPAIRED CARBON FIBER COMPOSITE MATERIALS WHICH HAVE BEEN MANUFACTURED IN AEROSPACE INDUSTRY

SÖNMEZ, Fikret Cem

Master, M.S. in Mechanical and Aeronautical Engineering

Supervisor: Assoc. Prof. Dr. Murat DEMİRAL

September, 2016, 57 pages

Advanced carbon fiber composites are becoming more important in the maintenance and used in a wider range of applications in aeronautical, marine, automotive, surface transport and sports equipments. Repair of these composite materials has always been an important challenge in aerospace structures. The repair must cover the service and specific requirement of the remaining life of the aircraft structure.

In my thesis, performance analyses of repaired carbon fiber composite materials were studied and compared with original ones. The entire test parts were manufactured from unidirectional carbon fiber materials. Fiber orientations were chosen as 0°-90°, 15°, 30°, 45°, and 60° vertical degrees. Each composite part was manufactured with 12 plies. 6 plies were removed and replaced on scarf repair operation. All the parts (original and repaired) were tested on tensile testing method and repair area was inspected by ultrasonic NDI method. After repair of our test parts, section of each ply orientation was examined with Scanning Electron Microscope (SEM). Test specimens were cleaned and coated with gold in a Polaron SC 502 sputter coater and examined with SEM in Gazi University, Department of Biology.

The result of this study revealed that the repair operations could affect the mechanical properties on the part. Designer and Material Review Board Engineers should make a strong analysis of the repair operation and its affects carefully.

Keywords: Composite repair, scarf repair, tensile strength of repaired part, composite materials, carbon fiber composite materials.



ÖZET

HAVACILIKTA KULLANILAN CARBON FIBER YAPILI KOMPOZİT MALZEMELERİN ONARIM SONRASI MEKANİK PERFORMANSLARININ ANALİZİ

SÖNMEZ, Fikret Cem

Yüksek Lisans, Makine ve Uçak Mühendisliği

Danışman: Doç. Dr. Murat DEMİREL

Eylül, 2016, 57 pages

Gelişmiş kompozit malzemeler her geçen gün üretim sektöründe kendine daha çok yer bulmaktadır. Havacılık, otomotiv, taşımacılık ve spor ürünleri de dâhil olmak üzere geniş bir kullanım alanına sahiptirler.

Havacılık sektöründe kompozit malzemelerin onarılması çok karşılaşılan bir durum olduğu gibi kompozit malzeme ile çalışmanın başlıca zorluklarından birisi olmuştur. Kompozit malzemenin kullanım alanının artması, kanat, silah sistemleri gibi kritik parçalarda da kullanılmaya başlanması ile birlikte onarım görmüş malzemelerin onarım sonrası mekanik davranışları ve dayanımları da gün geçtikçe daha çok önem kazanmıştır. Onarımlar uçağın ömrü boyunca orijinal malzeme ile aynı mekanik özellikleri sağlamalı ve bu özellikleri korumalıdır.

Bu tezin amacı, onarımların bu kadar kritik rol oynadığı havacılık sektöründe sıklıkla kullanılmakta olan karbon fiber kompozit malzemelerin onarım öncesi ve sonrası mekanik karakterlerini karşılaştırarak onarımın, özellikle havacılıkta çok kullanılmakta olan “Scarf” onarım tipinin mekanik özelliklere etkilerinin araştırılmasıdır.

Test parçası olarak tamamı tek yönlü dizilime sahip Karbon-Epoksi malzemedan, 0-90°, 15°, 30°, 45° ve 60° derece yönlerinde 12 katman dizilerek üretilmiştir. Fiber diziliminin değişken olarak belirleyici olmaması amacı ile dıştan içe 6 katman simetrik olarak dizilim tercih edilmiştir. Elimizde bulunan farklı

açılarda üretilmiş kompozit test numunelerinin yarısına onarım yapılmış, 6 katman derinliğe inen bir hasar simüle edilerek onarım yapılmıştır.

Üretilmiş olan kompozit malzemelerin onarım yüzeylerinden alınmış olan kesitler SEM (Scanning Electron Microscope) mikroskopunda 5-10 kV voltaj altında incelenmiş, gözlem ve tespitler tez içerisinde belirtilmiştir.

Tez sonuçları incelendiğinde karbon fiber yapılu kompozit malzemelerde yapılan onarımın parçanın mekanik özelliklerine doğrudan etki ettiği, dizayn ve onarımdan sorumlu mühendislerin analizlerini yaparken onarımın etkilerini özenle değerlendirmeleri gerektiği tespit edilmiştir.

Anahtar kelimeler: Kompozit malzemeler, karbon fiber kompozit malzemeler, scarf onarım, kompozit malzemelerde onarım.

CHAPTER ONE

INTRODUCTION

A composite material can be defined as a combination of a matrix and a reinforcement, which when combined gives properties superior to the properties of the individual components. In the case of a composite, the reinforcement is the fibres and is used to fortify the matrix in terms of strength and stiffness. The reinforcement fibres can be cut, aligned, placed in different ways to affect the properties of the resulting composite. The matrix, normally a form of resin, keeps the reinforcement in the desired orientation. It protects the reinforcement from chemical and environmental attack, and it bonds the reinforcement so that applied loads can be effectively transferred. Advanced composite and carbon fiber materials are becoming more important in the maintenance and used in a wide range of applications in aeronautical, marine, automotive, surface transport and sports equipment's. In the Aeronautical Industry; most of aircraft parts made from composite materials, such as elevators, landing gears, spoilers, wings and fuselages of aircrafts are manufactured from composite parts. New generation aircrafts like Boeings B787 Dreamliner and Airbus's A350 were designed with composite fuselage and wings structures. Main advantages of composite materials are high strength, long shelf life, relatively low weight, and strong corrosion resistance [2].

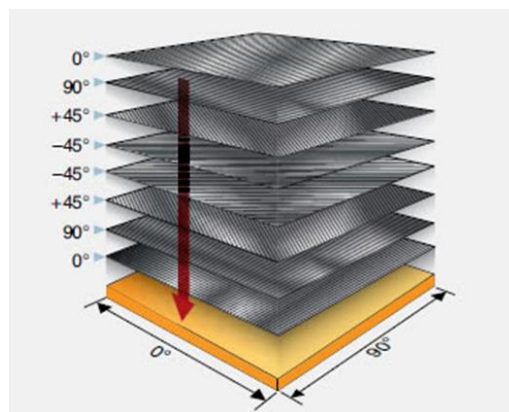


Figure 1.1: Composite materials.

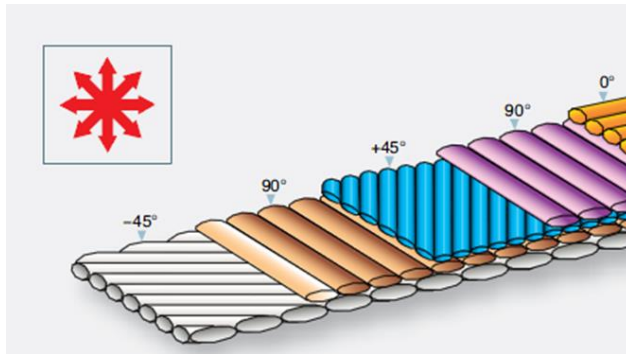


Figure 1.2: Composite materials.

The composite structures of interest are mainly components composed of laminated plies as shown in Figure 1.1. and Figure 1.2.

Composites are made up of individual materials referred to as constituent materials. There are two main categories of constituent materials: matrix and reinforcement. At least one portion of each type is required. The matrix material surrounds and supports the reinforcement materials by maintaining their relative positions. The reinforcements impart their special mechanical and physical properties to enhance the matrix properties. A synergism produces material properties unavailable from the individual constituent materials, while the wide variety of matrix and strengthening materials allows the designer of the product or structure to choose an optimum combination [3].

Composites are strong, light weight structures well suited for aerospace applications. However, they are subject to nonconformances both during original fabrication and assembly.

Some nonconformances can happen during original part fabrication. These include resin rich surfaces, which are shown in the top two pictures on the left hand side of the slide. This excess resin on the surface is very brittle and can crack off during service and can lead to moisture ingress and further microcracking during the life of the part. This is typically reworked by sanding off the excess resin.

The opposite of this nonconformance is a resin poor surface where the fibers are exposed on the surface and there are small pits between the fibers.

Another nonconformance that can occur during original part fabrication is the FOD is cured into the part.

Laminate structures are assembled so that the fiber orientation provides most of the desired mechanical performance. The most important damage to composites is the result of impact effects.

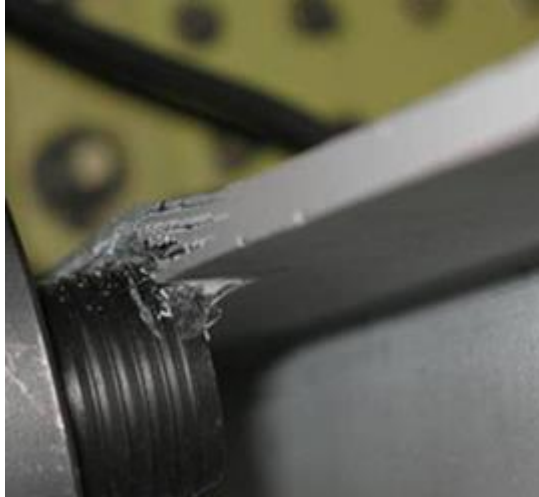


Figure 1.3: Impact damage example 1.

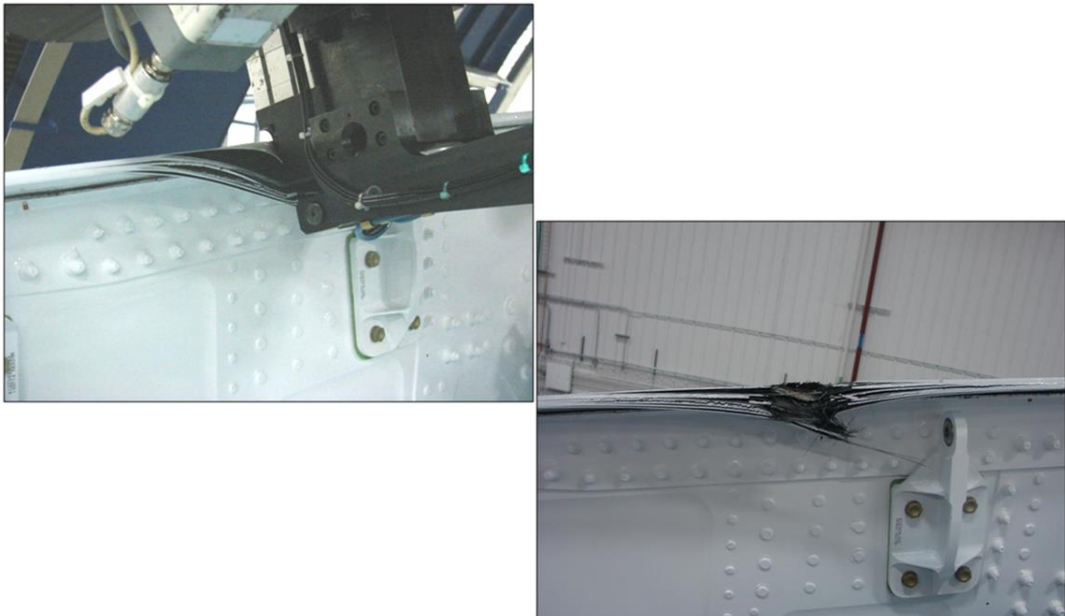


Figure 1.4: Impact damage example 2.

Impact energy is usually more extensive than metals. Some of the damage types on composite structures are shown in Figure 1.5

Figure 1.3. and Figure 1.4. are some of the examples to result of impact damage.

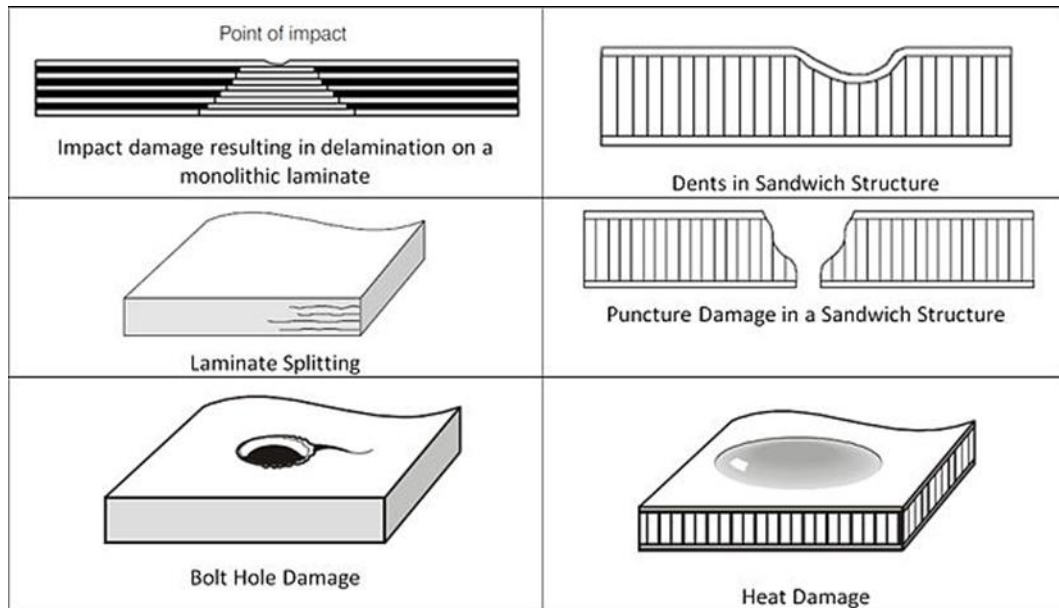


Figure 1.5: Damage types on composite structures [3].

1.1 Purpose

The purpose of this thesis study is to make mechanical performance analysis on repaired carbon-fiber composite materials which have been manufactured in aerospace industry. Carbon-fiber composite materials have been chosen as material type. Different orientation types will be used to create more examples to study different type of materials on same condition.

The goal of this study is to examine mechanical performance of repaired carbon fiber composite materials which are manufactured in aerospace industry. The nature of the topic dictates the analysis of different orientation types to create a variety of examples to study different types of materials in the same condition.

CHAPTER TWO

COMPOSITE MATERIALS

A composite material can be defined as a combination of two or more materials. Each material retains its separate chemical, physical and mechanical properties. The two constituents are reinforcement and a matrix which are made of metals, polymers and ceramics [4].

Continuous (UD, Cloth and Roving) reinforcement types are the most general one's on aerospace industry (Fig. 2.1).

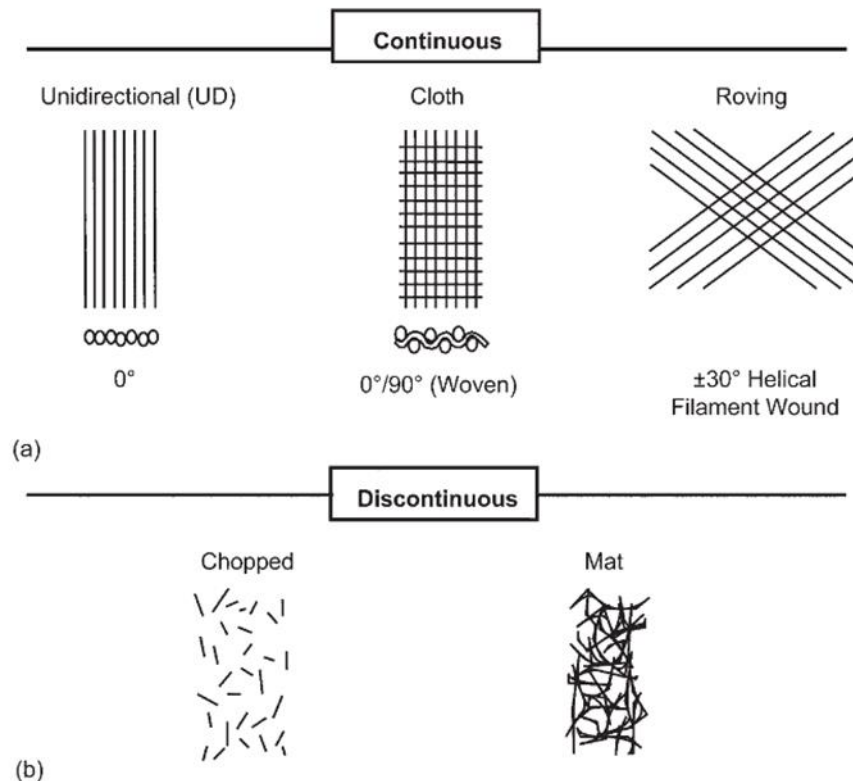


Figure 2.1: General reinforcement types.

Continuous fibers have proportional relation between width and height. Continuous-fiber composite materials have prearranged orientation but discontinuous

fibers generally have a random orientation. Examples of continuous fiber orientation shown on Figure 2.1(a) and also discontinuous reinforcements are shown on Figure 2.1(b). Continuous-fiber composites are generally made by laminates by stacking single sheets of continuous fibers in different orientations.

Fibers has small diameter, result of this always produce high-strength. High-strength carbon fiber materials have greater flexibility and are more suitable to manufacture processes.

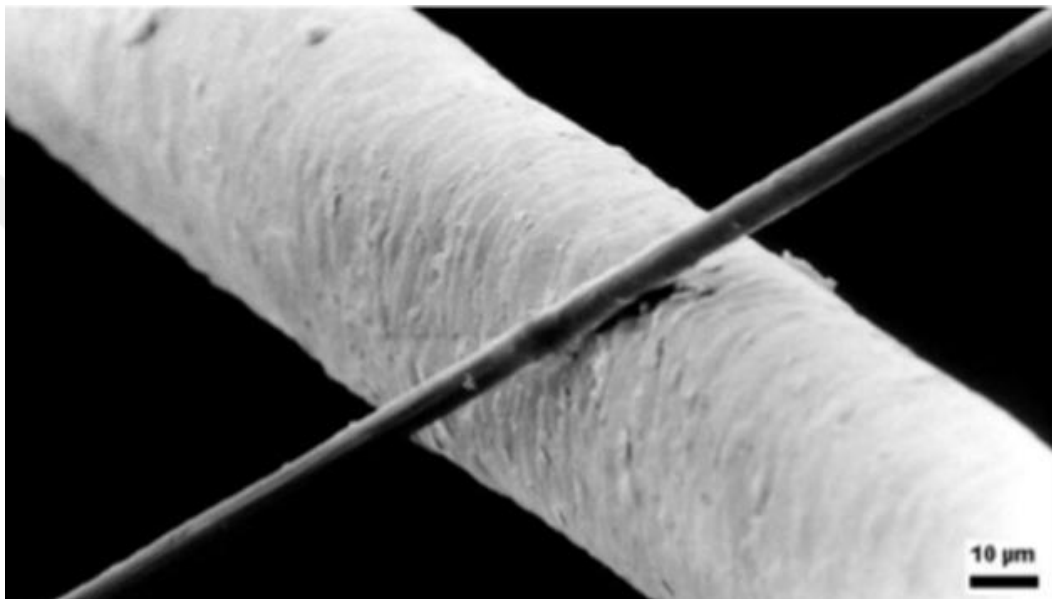


Figure 2.2: Compare of a human hair and carbon-fiber.

Common composite materials can be classified as follows [5] (based on form of reinforcement):

1. Carbon fibers as the reinforcement (Fibrous Composites):
 - a. Random fiber (short fiber) reinforced composites

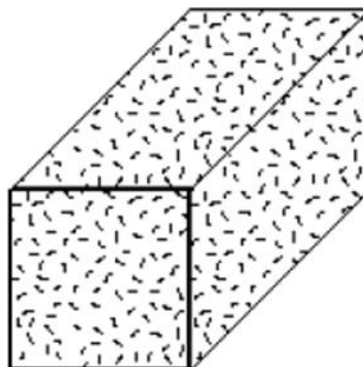


Figure 2.3: Random fiber composites.

b. Continuous fiber (long fiber) reinforced composites

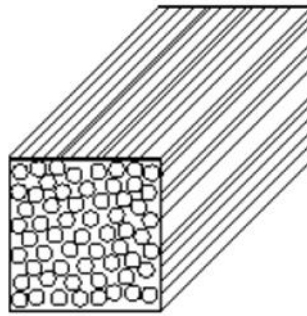


Figure 2.4: Continuous fiber composites.

2. Particles as the reinforcement (Particulate composites):

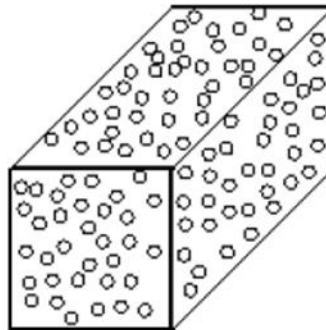


Figure 2.5: Particulate composites.

3. Flat flakes as the reinforcement (Flake composites):

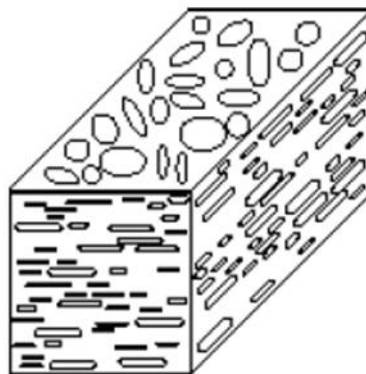


Figure 2.6: Flake composites.

4. Fillers as the reinforcement (Filler composites):

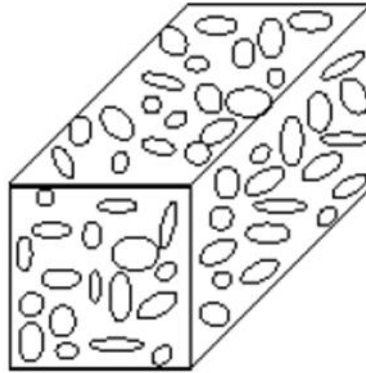


Figure 2.7: Filler composites.

A compare on advantages and disadvantages of composite parts and metallic parts is below [6]:

2.1 Compare of Advantages of Composite Materials and Metallic Parts:

- i) Advantages of metallic parts:
 - a) Shelf life is longer than composites.
 - b) Properties and special characters of materials well known.
 - c) High coefficient of thermal expansion.
- ii) Advantages of composites:
 - a) Light weight.
 - b) Better corrosion resistant.
 - c) Better fatigue resistant.
 - d) High stiffness.
 - e) Easy to give form to material.
 - f) Easy to use on curved surfaces.

2.2 Compare of Disadvantages of Composite Materials and Metallic Parts:

- i) Disadvantages of metallic parts:
 - a) Metallic parts have more sensitive surface treatment.
 - b) Corrosion and fatigue resistant worse than composites.
 - c) Difficult to form.
- ii) Disadvantages of metallic parts composite:

- a. More expensive than metallic parts.
- b. Short shelf life

2.3 General Advantages of Composite Materials

The best known advantage of composite materials is weight saving. The best way to understand this advantage is to check strength to weight ratio between composites and other type of materials.

For a new design, the material should be strong enough to withstand the loads. If the material which is on the design is not strong enough this may cause big problems on aerospace industry. Increase of the bulk and weight of the part or make a change on design and material is the best way to make a good design [7].

In the aerospace industry, working with the close tolerances is very important for the design and safety. It is not so hard to achieve close tolerances on composite parts.

Composites always have higher impact damage resistance because of internal form. Impact resistance and other mechanical specialties are changed by fiber orientation pattern.

2.4 Carbon Fiber

Carbon fibers named fiber materials which have at least 92 wt. % carbons in composition [8, 9]. Because of high fatigue strength carbon fibers are very common in aircraft components [10, 11]. Carbon Fiber consist a fibers its diameter about 5–10 μ m and composed mostly of carbon atoms. Carbon fiber composites are real hi-tech materials which provide better structural properties. Carbon fiber's tensile strength is almost 3 times bigger than steel in 4.5 times less dense.

CHAPTER THREE

REPAIR OF COMPOSITE MATERIALS

Rapid increase in application of composites in commercial and military aerospace applications has led to increased interest in composite repair technologies [12].

Usage of composites parts in commercial and especially aeronautical industry increasing. Repairs are always major challenges for the composite materials in aerospace structures. Composite materials have a common usage in structures (fairings, doors, weapon systems, wings.). In these applications if a repaired structure fails, worst case the aircraft operation would be affected and result could be catastrophe. The repair must cover the service and specific requirement of the remaining life of the aircraft structure [13, 14].

Bonded scarf or stepped repairs are preferred methods of repairing composite structures to have high strength recovery is needed. Especially scarf repairs are the common repair method to meet the flushness requirements for aerodynamic surfaces. For critical parts and structures, scarf repairs may be the only available solution to avoid component replacement which may affect the cost.

Bonded scarf or stepped repairs are used in composite structures when high strength recovery is needed or when there is a requirement for a flush surface to satisfy aerodynamic or stealth requirements. Scarf repairs are complex to design and require the removal of significant parent structure, particularly for thick skins [34].

Reinforcing patch repairs are aimed at restoring the load path in the parent structure removed by the damage, without significantly changing the original strain distribution. Significant damage in case of metals includes exfoliation corrosion and fatigue or stress-corrosion cracking, and in the case of composites includes: delaminations, fibre failures and heat damages. The following is a partial “Check List” of requirements which need to be demonstrated in the certification of critical repairs [14]:

- a) Restoration of residual strength
- b) Prevent or slow growth of residual damage—if remaining in the structure
- c) Minimum change in local stiffness or stress distribution
- d) Very low probability of failure (or high durability) in the stress, chemical and thermal environment experienced by the airframe
- e) Tolerance to potential mechanical damage
- f) Proof of satisfactory design and implementation—suitable quality control tracking procedures
- g) No unforeseen consequences: aerodynamic, flutter or clearance

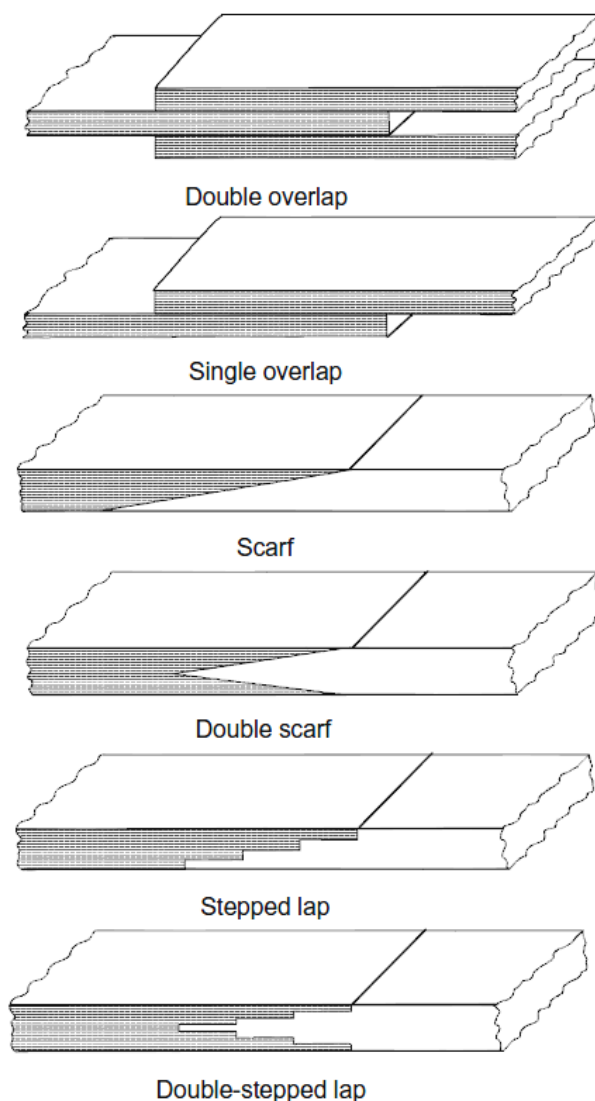


Figure 3.1: Main types of joint configuration used for repairs to composite structure.

Figure 3.1 shows different types of repairs. There are a lot of types of repairs on aviation industry but most common used is scarf repairs.



Figure 3.2: Repair types and repetitiveness table.

3.1 Scarf Repair

Scarf repair reconstructs full structural and mechanical characteristics like before repair. Each ply of the carbon fiber laminate is removed ply by ply from the damage area and replaced with reinforcement plies.

Compare to other repair types scarf repairs comparatively have better surface profile performance. To maintain flush surfaces after repair and minimize the change in surface profile, an additional 1 extra sanding layer usage is very common on aerospace industry.

The bonded repair should restore the original stiffness, static strength, durability and damage tolerance. Creep of moisture laden adhesive under high temperature loading also needs consideration. Common bonded repair designs performed on the aircraft structure may be limited to options such as an external doubler, step-lap or scarf repair (Fig. 1). The bonded doubler strength may be compromised by geometrically non-linear bending, which increases the stress concentration adjacent to the damage cut-out region. By contrast, the scarf or step-lap configuration should minimise secondary bending effects, but will be more difficult to apply [17].

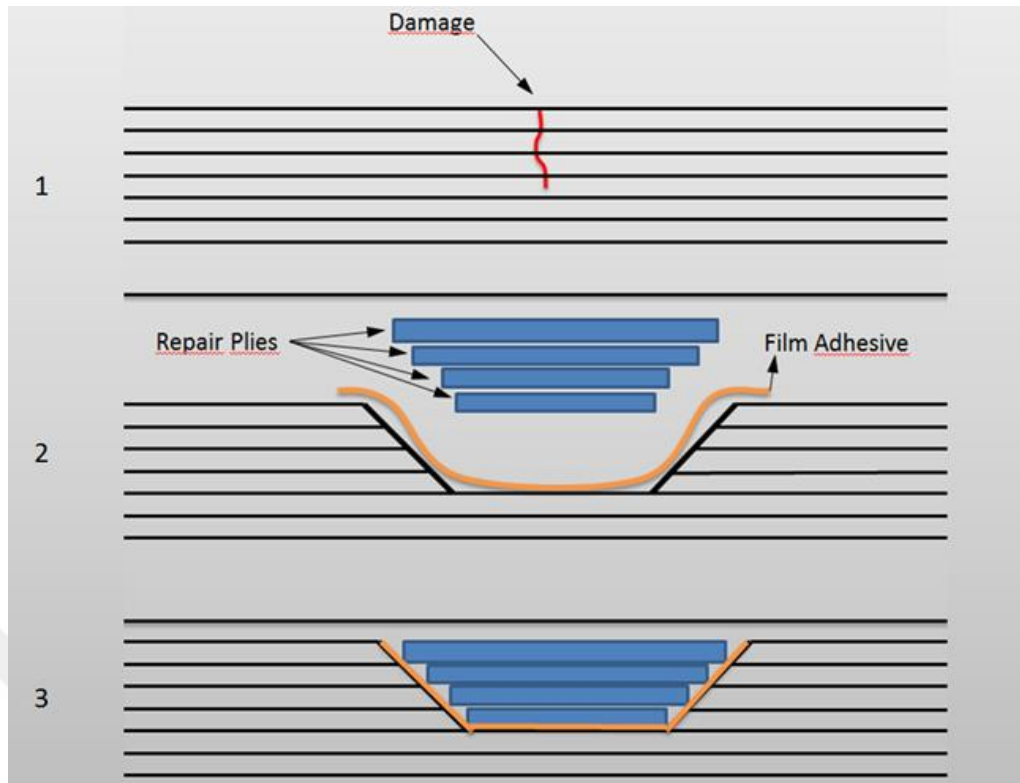


Figure 3.3: Scarf repair.

Bonded scarf repair should restore the original damage tolerance [17, 19, 20]. To produce the original parts characteristics ply orientation of the repair surface should be same as the original removed plies.

Bonded scarf repairs and stepped repairs are preferred when;

- a. High strength recovery is needed.
- b. Flush surface is needed to obtain aerodynamic surface [21].

Repair must demonstrate damage tolerance as well. The research's shows that scarf repaired composites have higher damage tolerances and better impact performance [12].

Scarf repair steps are shown below:

- 1) Inspection and mapping of damage:

The size and depth of damage to be repaired must be observed using nondestructive control (NDI) method. As a result of NDI Inspection delamination/damage and delamination depth below the surface and damage width composites will be discovered. One of the popular techniques is tap testing shown on Figure 3.3, tap inspection is used with a lightweight object, such as a coin or hammer, is used to locate damage. Advantages of tap inspection are; it is simple and

it can be used to rapidly inspect large surfaces. Tap testing generally used to detect delamination damage close to the surface. Ultrasonic can be used to detect delamination and damages located deep below the surface.

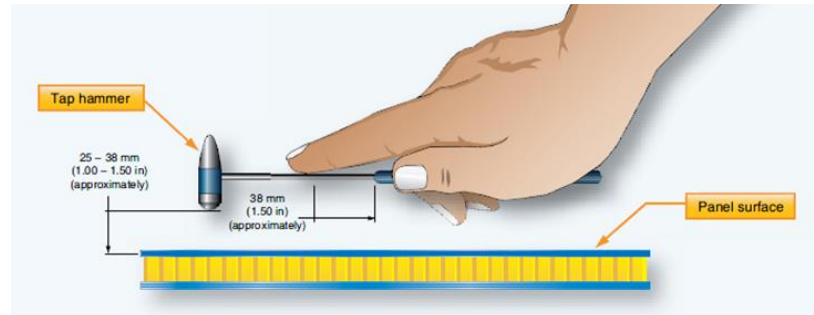


Figure 3.4: NDI method - tap inspection.

2) Removal of Damaged Material:

After the damaged area has been determined, the damaged laminate must be removed. The taper remove (scarf angle) should be less than 5° to minimize the shear strains along the bond line.

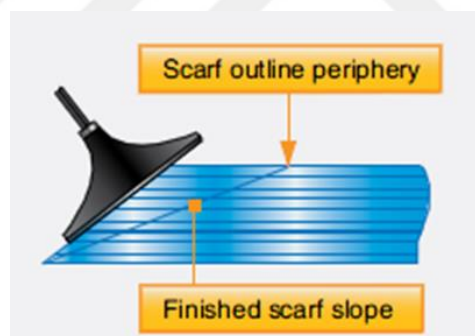


Figure 3.5: Taper remove of laminates.

3) Surface Preparation:

The laminate close to the scarf zone should be abraded with using sandpaper and it should be cleaned with solvent or clean water.

4) Laminating:

Selection of the reinforcing material is very critic to ensure the repair surface and layers to have acceptable mechanical performance. The reinforce layers fiber orientation should match with the original part laminate layers orientation. By this way mechanical properties of the repair area will have close mechanical properties as original part.

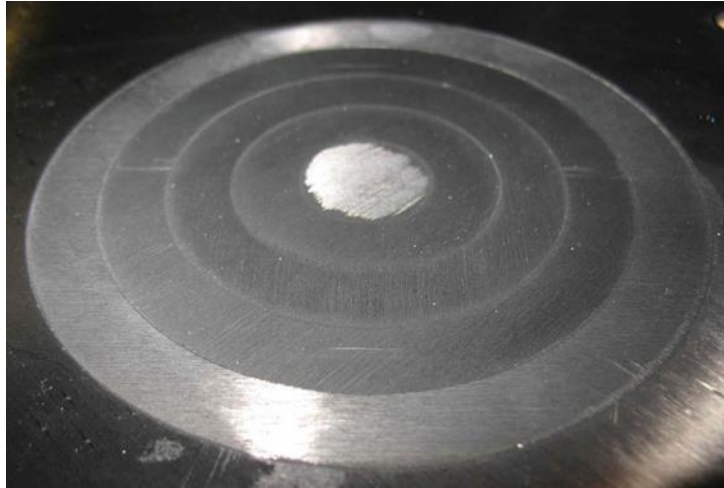


Figure 3.6: Scarf Repair taper laminate removal example 1.

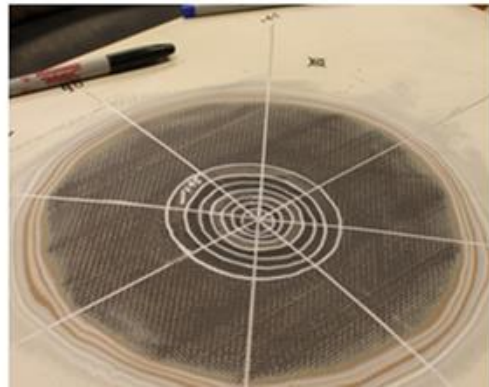


Figure 3.7: Scarf Repair taper laminate removal example 2.

Scarf repairs are the most invasive repairs performed on a composite part.

The Figure 3.7. on the left picture shows the scarfing, or taper sanding, process where a large amount of auto-clave cured material is being removed around the damaged area. The image on the right shows the final scarf with the ply outlines highlighted. After this step, the repair plies will be cut out of new material, laid up onto the part, and cured onto the part to form the repair.

CHAPTER FOUR

TEST METHODS

Nondestructive test (NDT) methods may rely upon use of electromagnetic radiation, sound, and inherent properties of materials to examine test specimens. Ultrasonic NDT method used to check the test parts and repairs for my study.

4.1 Nondestructive Inspection

The terms Nondestructive Examination (NDE), Nondestructive Inspection (NDI), and Nondestructive Evaluation (NDE) are also commonly used to describe these inspection methods. Common nondestructive methods are ultrasonic, magnetic particle, liquid penetrant, radiographic, remote visual inspection (RVI), eddy current testing.

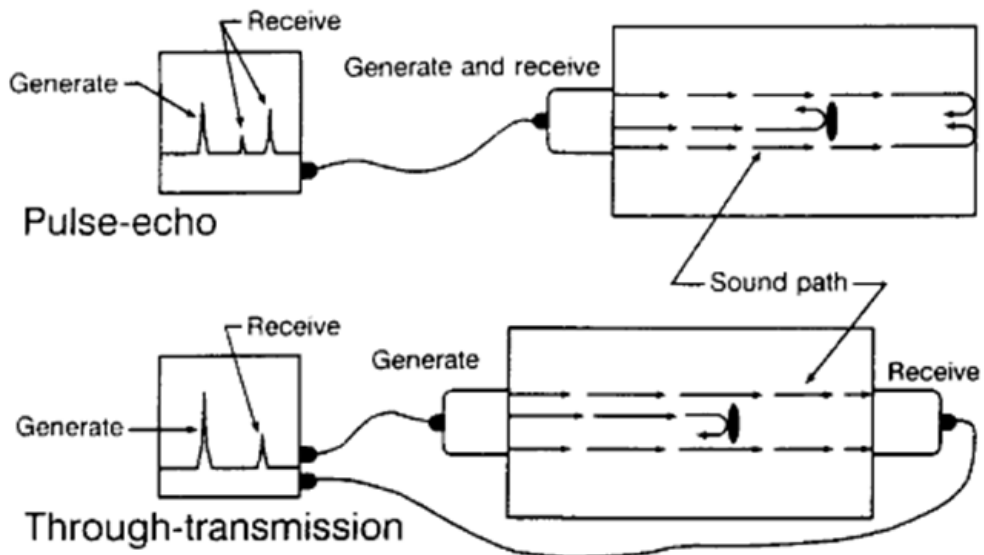


Figure 4.1: Ultrasonic inspection.

Ultrasonic inspection is an NDI technique that uses sound energy moving through the test specimen to detect discrepancies. Sound energy passing through the specimen and displayed on a computer data program.

4.1.1 Through Transmission Inspection

This inspection employs two transducers, one to generate and a second to receive the ultrasound. A defect in the sound path between the two transducers will interrupt the sound transmission. The magnitude (the change in the sound pulse amplitude) of the interruption is used to evaluate test results. Through transmission inspection is less sensitive to small defects than is pulse-echo inspection.

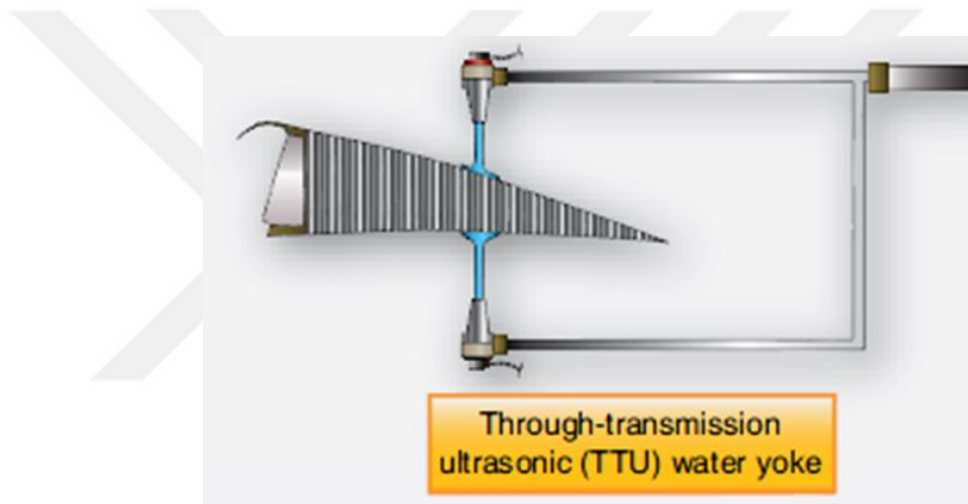


Figure 4.2: NDI method – TTU inspection.

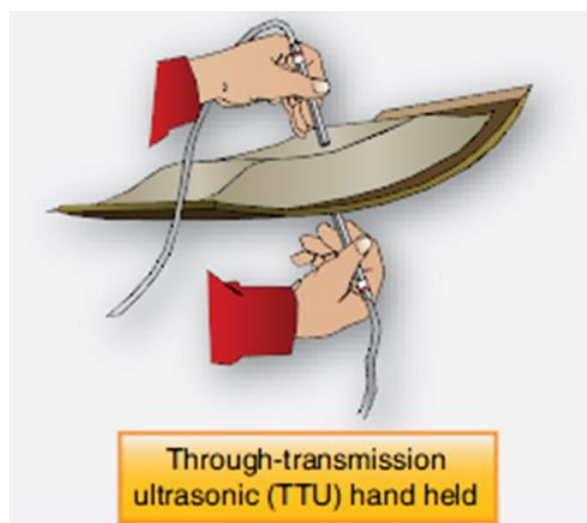


Figure 4.3: NDI method – manual TTU inspection.

4.2 Destructive Inspection

4.2.1 Tensile Test

A tensile test, also known as tension test, is probably the most fundamental type of mechanical test you can perform on material. Tensile tests are simple, relatively cheap, and standardized. By pulling on something, you will very quickly determine how the material will react to forces being applied in tension. As the material is being pulled, you will find its strength along with how much it will elongate.

You can learn a lot about a substance from tensile testing. As you continue to pull on the material until it breaks, you will obtain a good, complete tensile profile. A curve will result showing how it reacted to the forces being applied. The point of failure is of much interest and is typically called its "Ultimate Strength" or UTS on the chart.

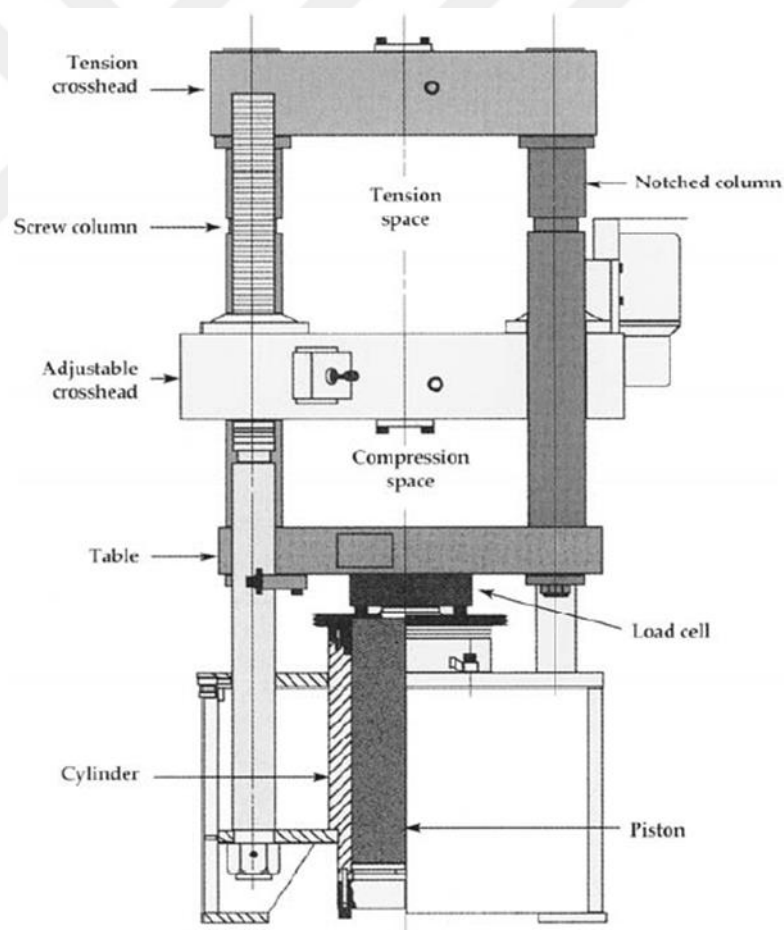


Figure 4.4: Universal tensile test machine.

Testing machines can be electromechanical or hydraulic. Electromechanical machines are based on an electric motor which can be adjustable. Motion loads the specimen in tension. Speed can be changed by changing the speed of the motor. Hydraulic testing machines are based on a single or dual-acting piston that moves the load up or down. In a manual operated tensile testing machine, operator adjusts the pressure-compensated the valve to control the rate of loading.

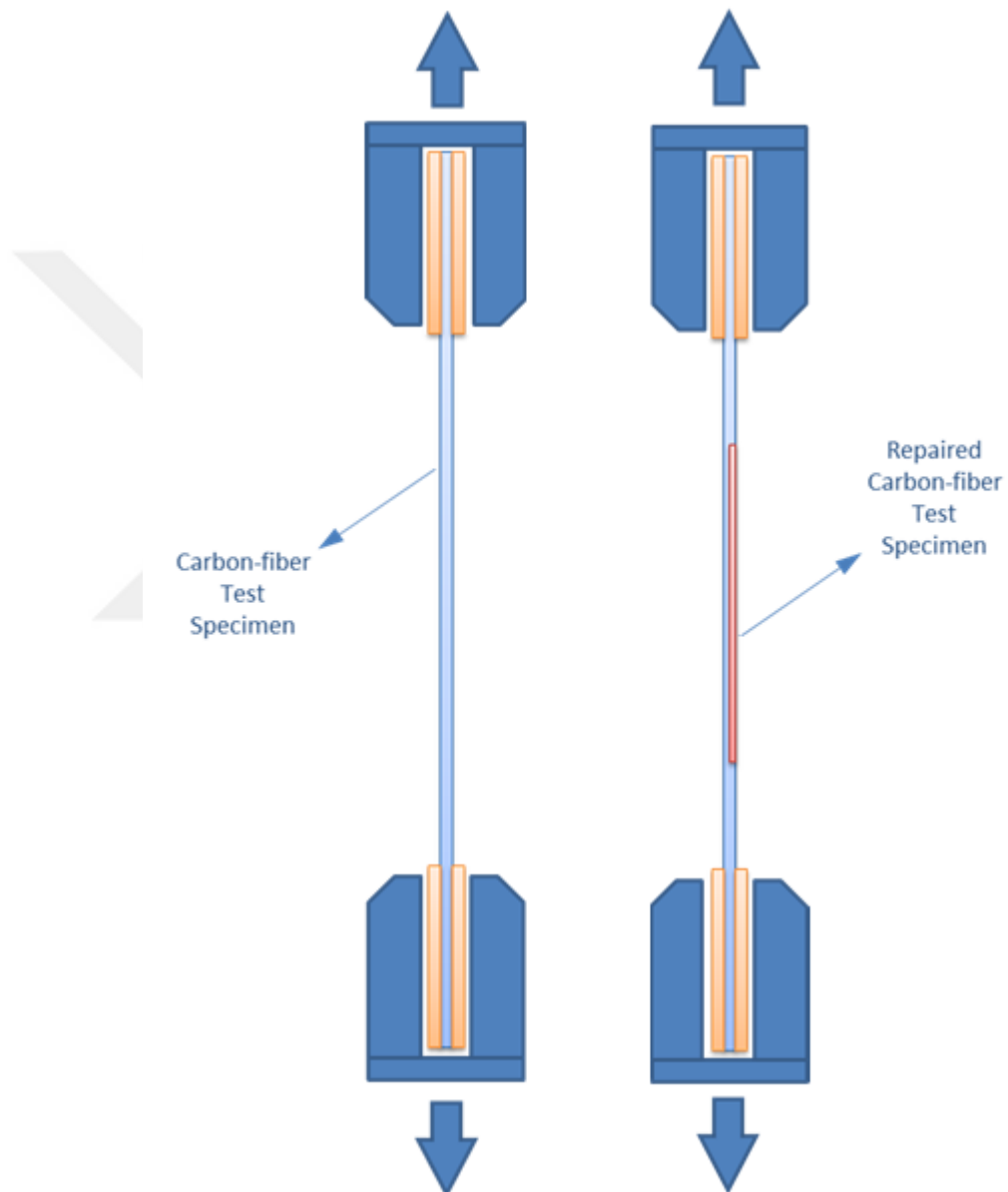


Figure 4.5: Tensile test.

CHAPTER FIVE

EXPERIMENTAL DATA

Carbon-epoxy ABS5139C1219A (AIMS 05-01-001) composite materials were selected for this study [22]. The DA4-653-5 [23] adhesive film, which is an adhesive very commonly used in the structural applications of aerospace and aircraft components, was chosen.

5.1 Test Specimens

The ply orientation prepared for each of the test specimens have been shown as follows:

5.1.1 Ply Orientation of the 0-90-Degree Test Specimens

Ply orientation of the 0-90-degree test specimens $[(0/+90)_3(+90/0)_3]$

Table 5.1: Ply orientation of the 0°-90° test specimens.

Ply Number	Ply Angle
1	0
2	90
3	0
4	90
5	0
6	90
7	90
8	0
9	90
10	0
11	90
12	0

5.1.2 Ply Orientation of the 15-Degree Test Specimens

Ply orientation of the 15-degree test specimens $[(+15/-15)_3(-15/+15)_3]$

Table 5.2: Ply orientation of the 15° test specimens.

Ply Number	Ply Angle
1	15
2	-15
3	15
4	-15
5	15
6	-15
7	-15
8	15
9	-15
10	15
11	-15
12	15

5.1.3 Ply Orientation of the 30-Degree Test Specimens

Ply orientation of the 30-degree test specimens $[(+30/-30)_3(-30/+30)_3]$

Table 5.3: Ply orientation of the 30° test specimens.

Ply Number	Ply Angle
1	30
2	-30
3	30
4	-30
5	30
6	-30
7	-30
8	30
9	-30
10	30
11	-30
12	30

5.1.4 Ply Orientation of the 45-Degree Test Specimens

Ply orientation of the 45-degree test specimens $[(+45/-45)_3(-45/+45)_3]$

Table 5.4: Ply orientation of the 45° test specimens.

Ply Number	Ply Angle
1	45
2	-45
3	45
4	-45
5	45
6	-45
7	-45
8	45
9	-45
10	45
11	-45
12	45

5.1.5 Ply Orientation of the 60-Degree Test Specimens

Ply orientation of the 60-degree test specimens $[(+60/-60)_3(-60/+60)_3]$,

Table 5.5: Ply orientation of the 60° test specimens.

Ply Number	Ply Angle
1	60
2	-60
3	60
4	-60
5	60
6	-60
7	-60
8	60
9	-60
10	60
11	-60
12	60

5.2 Manufacturing Data for the Test Specimens

The laying-up process was completed inside a clean room where there was temperature and humidity control. The temperature was 21°C and the humidity was 45%. The UD Prepreg lay-up process was completed in accordance with the orientations that have been given in Figure 5.1. After the lay-up process was completed on all of the test specimens, they were prepared for the autoclave cure.

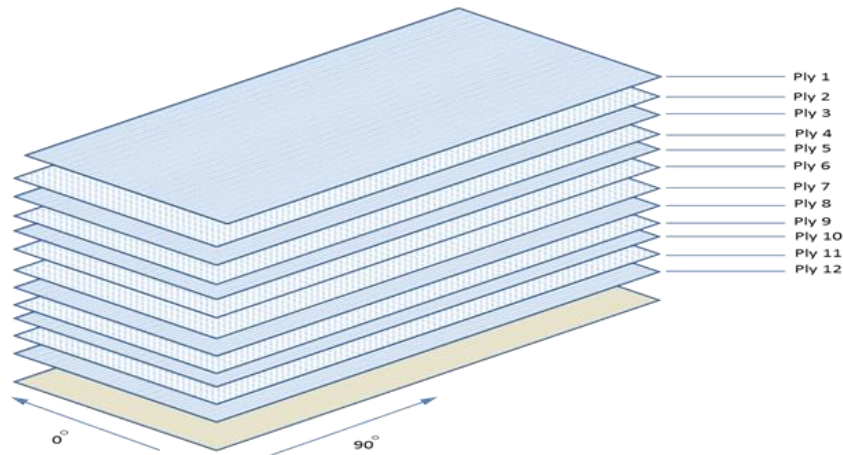


Figure 5.1: Ply sequence of the test specimens.

The autoclave cure operation was completed with the values given below:

Cure temperature (°C): 180 ± 5

Pressure (bar): $6.5 \pm .30$

Hold time (min): 120-190

Heat up rate (°C/min): 0.5-3.5

Cooling down rate (°C/min): 0.5-3.5

All of the information on temperature and pressure for the curing operation has been given in Figure 5.3.

Two each pieces of the test specimens from all orientations and in the dimensions of 200 mm x 270 mm have been cured in the autoclave. Each of the two test specimen scarves were repaired according to Chapter 51-77-12 of the AIRBUS Industry Structural Repair Manual. The 6 plies removed from the center of the part and the laying-up process of the repair/reinforcement plies have been completed according to the original ply orientation. Four pieces of glass fiber tabs were located in accordance with the DIN 2561 tensile test specifications. The tabs and repair plies were cured in the autoclave on the same cure cycle.

After all of the parts were cured, the waterjet cut method has been preferred to avoid any defects on the parts.

The nondestructive inspection was completed and no defects were observed on the test specimens. The final view of the test specimens has been given in Figure 5.2.

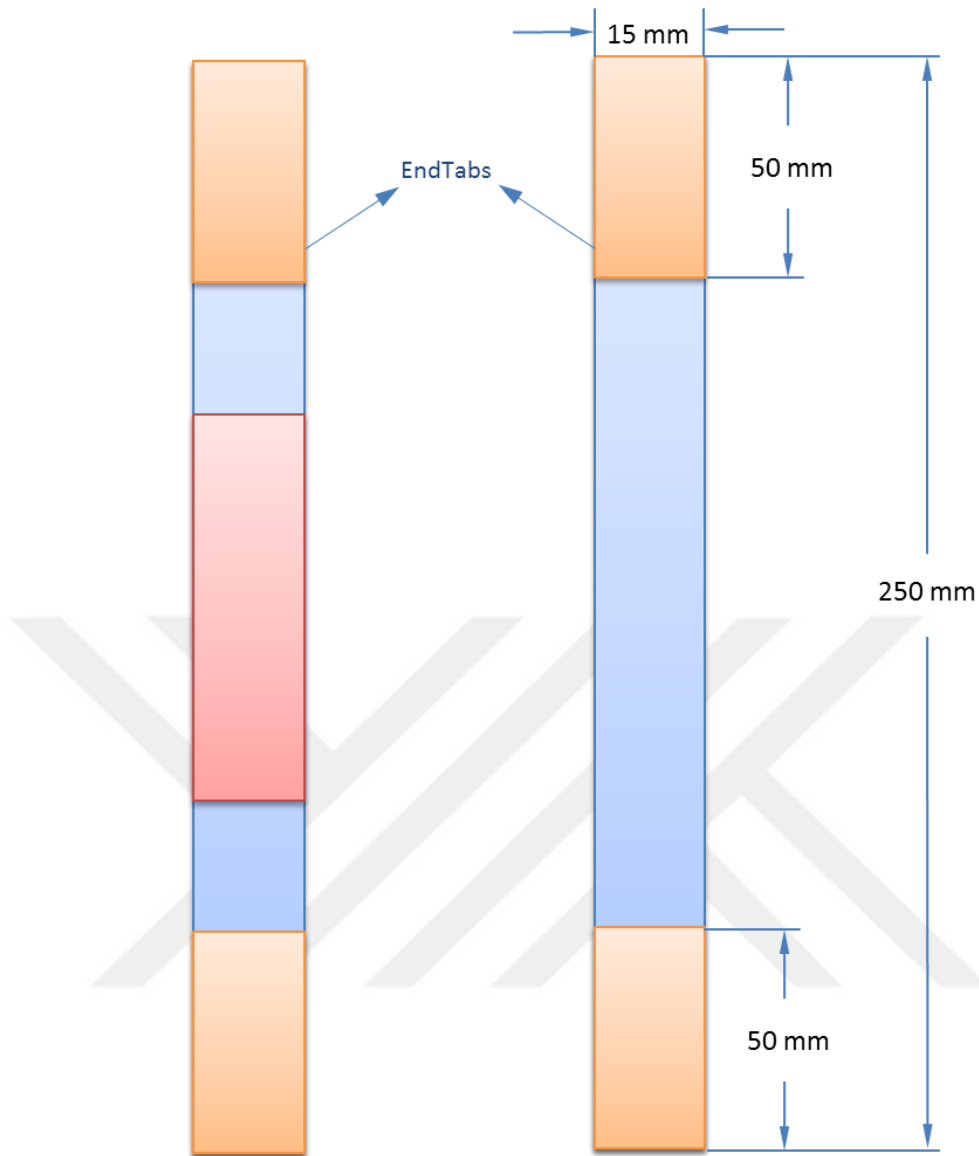


Figure 5.2: Test specimens.

The dimensions of the test specimens were prepared in accordance with the DIN 2561 standards.

5.2.1 Autoclave Report

Every step of the manufacturing process has been recorded and controlled for obtaining applicable specimens. The autoclave/cure process is very important for the manufacturing process and should be completely under control. Five thermocouples were used to chart the pressure/temperature changes. The records of the thermocouples for pressure and temperature have been given in Figure 5.3. below:

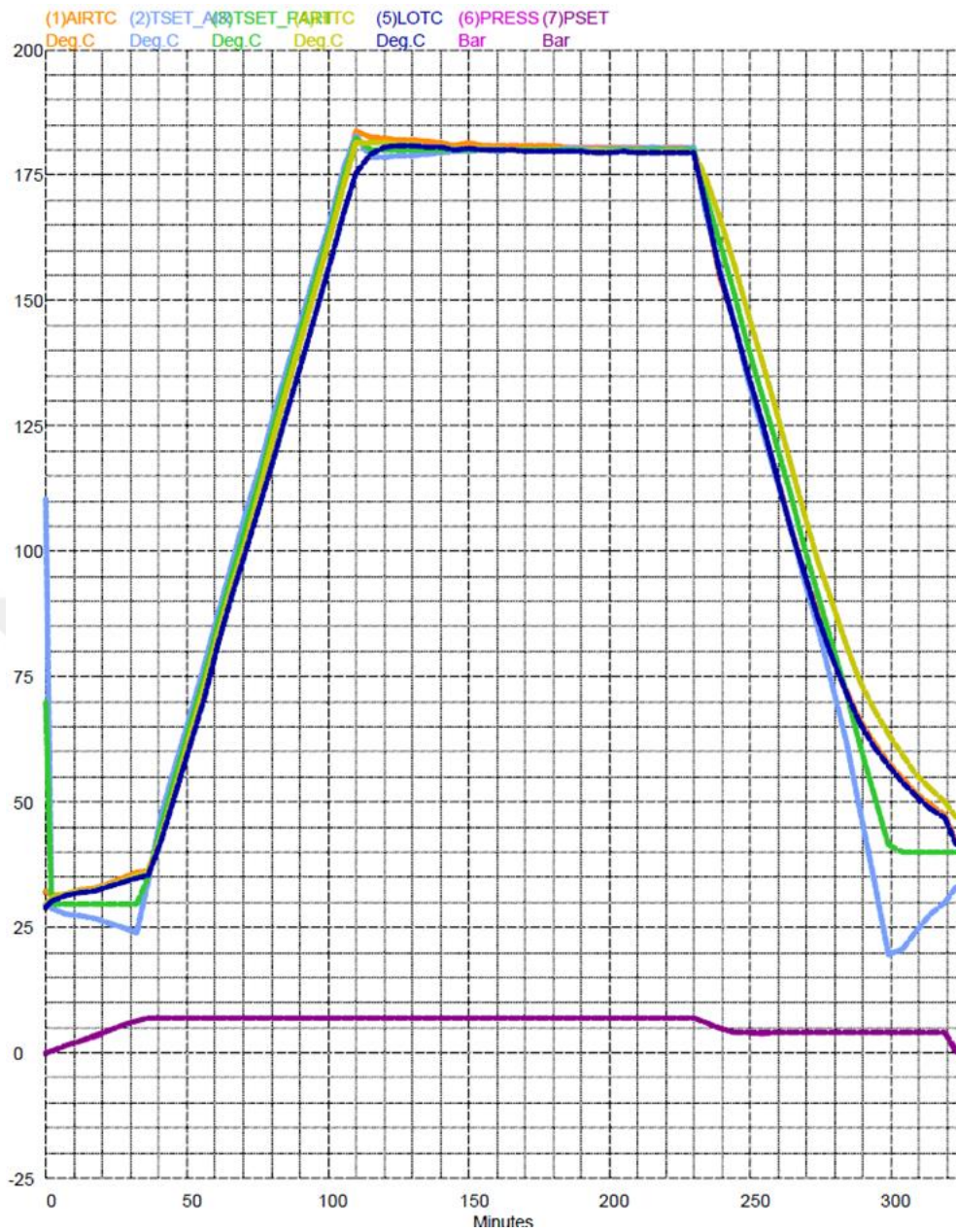


Figure 5.3: Pressure/Temperature diagram.

CHAPTER SIX

RESULT & ANALYSIS

After completion of the tensile tests, the results were compared and analyzed. Over 50 pieces of different test specimens were examined. All of the breakage points, the maximum tensile stress load at break and comparison of the different ply orientations were examined. Elasticity, yield strength and maximum tensile strengths are the most important parameters for comparison in the test specimens.

6.1 Tensile Test Results for the Repaired Test Specimens

6.1.1 Tensile Test Results for the 0°-90° Test Specimens

Four pieces from the 10 test specimens were chosen to show on the stress/strain graph (Figure 6.1). The results are those that are the closest to the average. All of the results have been given in Table 6.1.

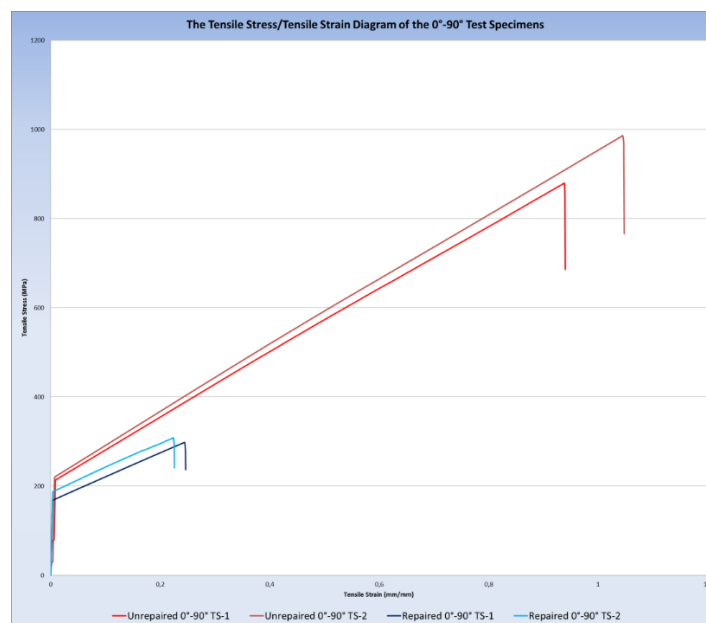


Figure 6.1: Four pieces from the 0°-90° test specimens in the tensile stress/tensile strain graph.

Table 6.1: The tensile test results for the 0°-90° test specimens.

	Maximum Tensile Stress [MPa]		Maximum Tensile Stress [MPa]
Repaired TS-1(0°-90°)	272	Unrepaired TS-1(0°-90°)	887
Repaired TS-2(0°-90°)	299	Unrepaired TS-2(0°-90°)	880
Repaired TS-3(0°-90°)	304	Unrepaired TS-3(0°-90°)	902
Repaired TS-4(0°-90°)	311	Unrepaired TS-4(0°-90°)	904
Repaired TS-5(0°-90°)	343	Unrepaired TS-5(0°-90°)	912

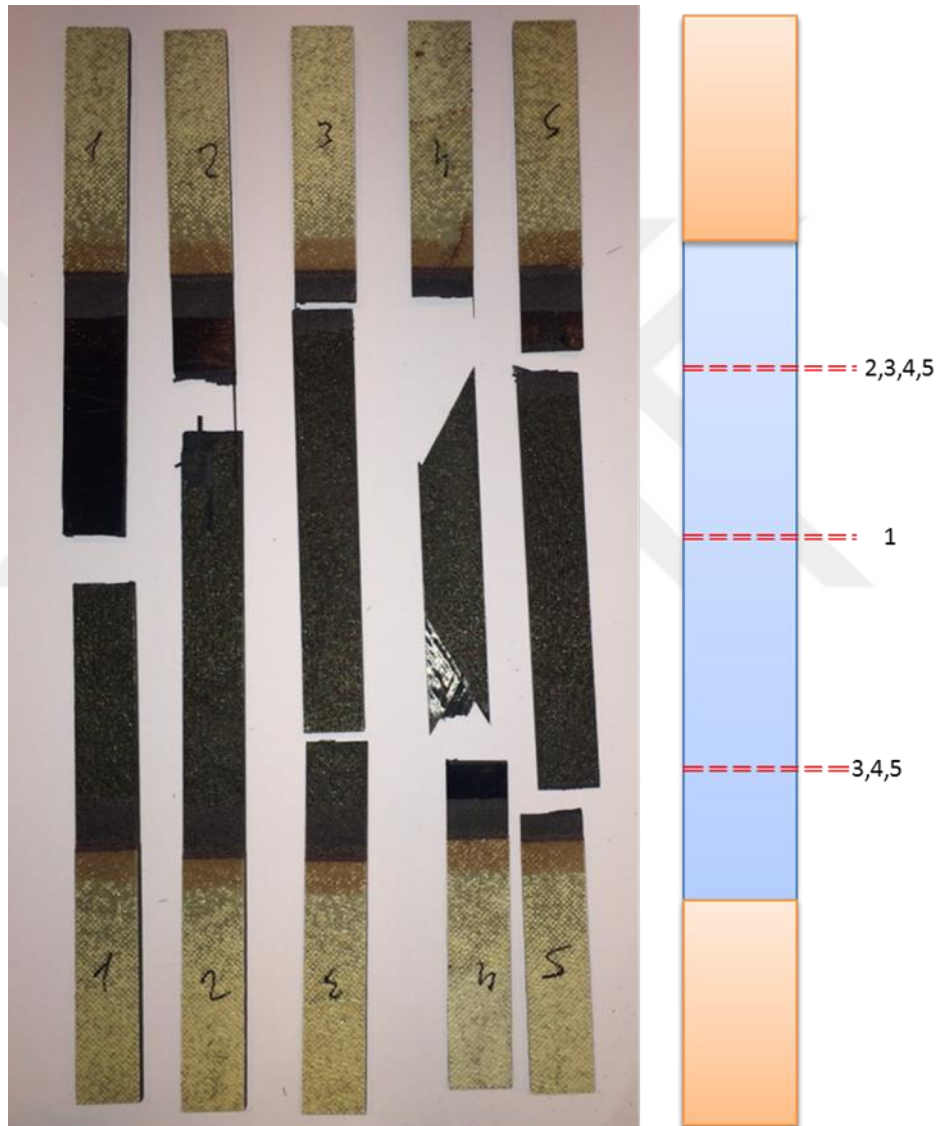


Figure 6.2: The unrepaired 0°-90° test specimens after the tensile test.

The maximum tensile stresses of the test specimens were measured between 880 MPa and 912 MPa (Table 6.1). As shown in Figures 6.2 and 6.3., the breakage angles were the same as the lay-up orientations.

When a small analysis was made between the repaired and the unrepaired 0°-90° test specimens, it can easily be said that the unrepaired original parts had stronger tensile stress resistances (Table 6.1).

It was observed that the repaired 0°-90° test specimens had a 3 times larger tensile resistance compared to the 15° test specimens (Tables 6.1 and 6.2). The maximum tensile stresses measured for the repaired 0°-90° test specimens were between 272 MPa and 343 MPa (Table 6.1). The results showed that cracks started from the edges of the repair surface (Figure 6.4).

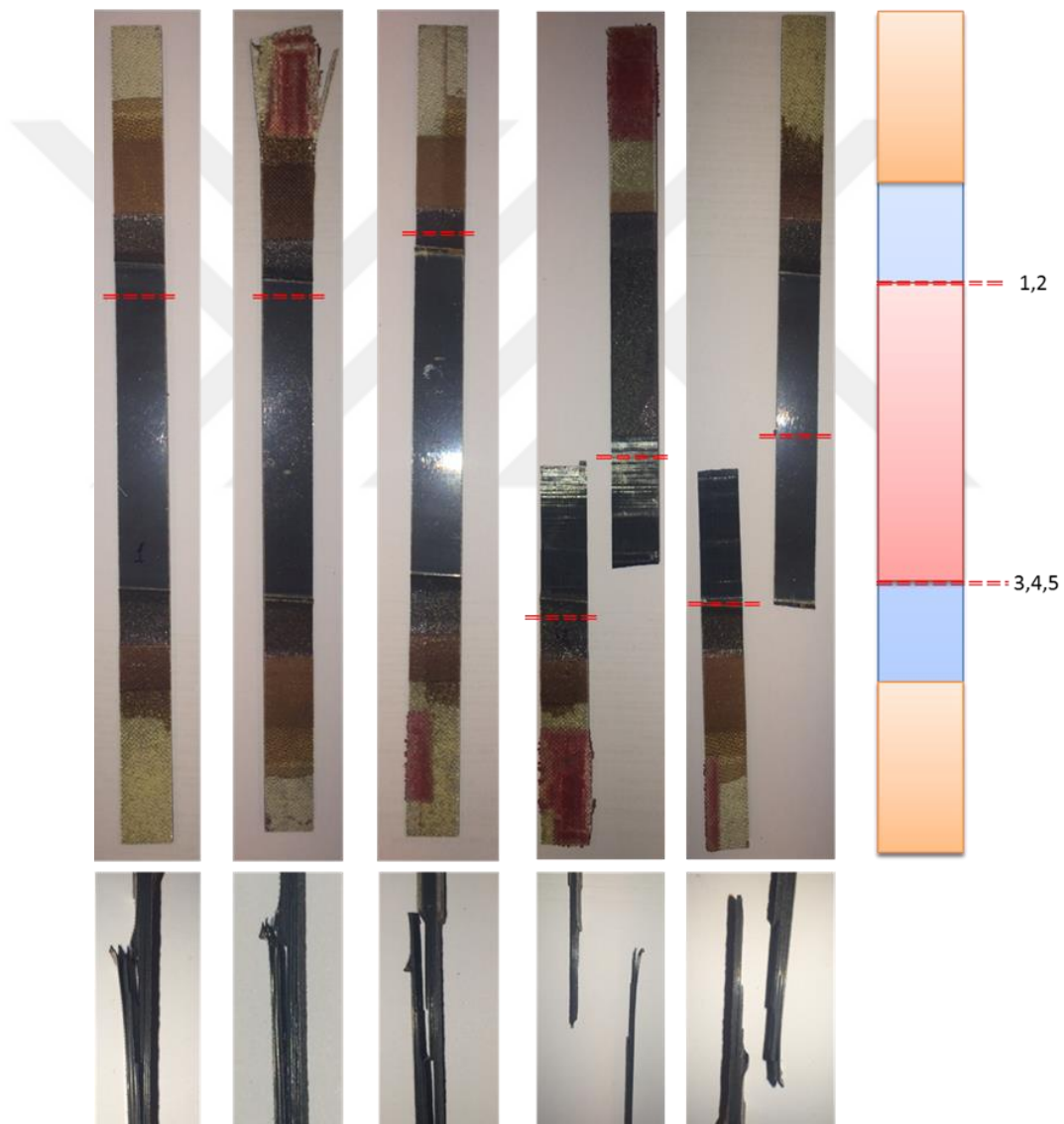


Figure 6.3: The repaired 0°-90° test specimens after the tensile test.

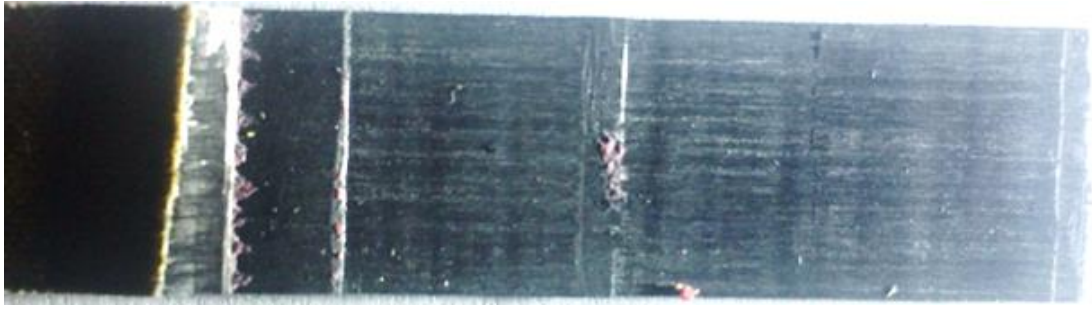


Figure 6.4: The repair plies of the 0°-90° test specimens.

The yield point of the unrepaired 0°-90° test specimens was higher than the repaired test specimens as it was given in Figure 6.5. The unrepaired (original) test specimens showed slightly stiffer properties than the repaired specimens on the 0°-90° lay-up carbon fiber composite materials.

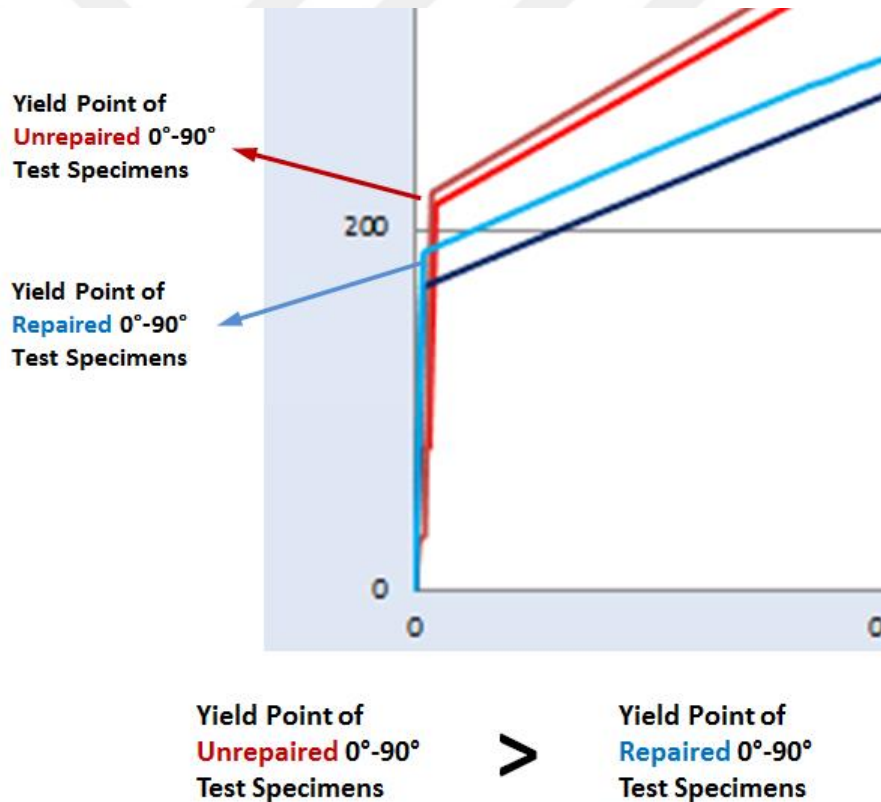


Figure 6.5: The yield strength points of the 0°-90° test specimens.

The scanning electron microscope (SEM) examinations for the 0°-90° test specimens:

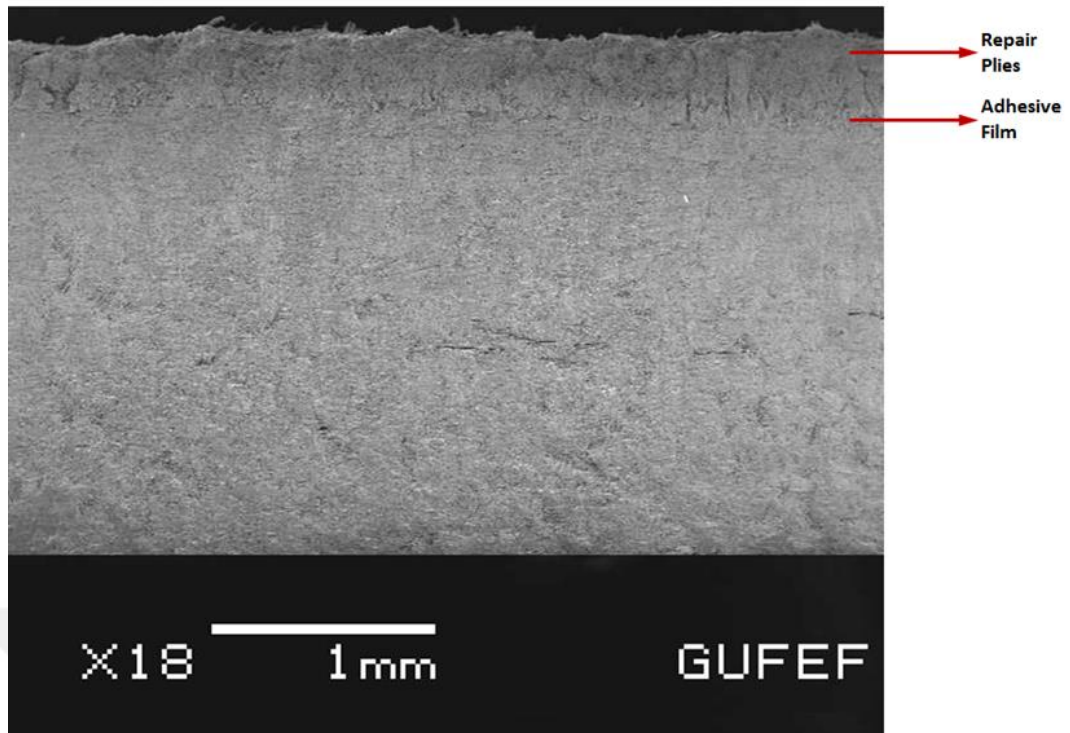


Figure 6.6: The SEM view 1.1 for the 0°-90° test specimens.

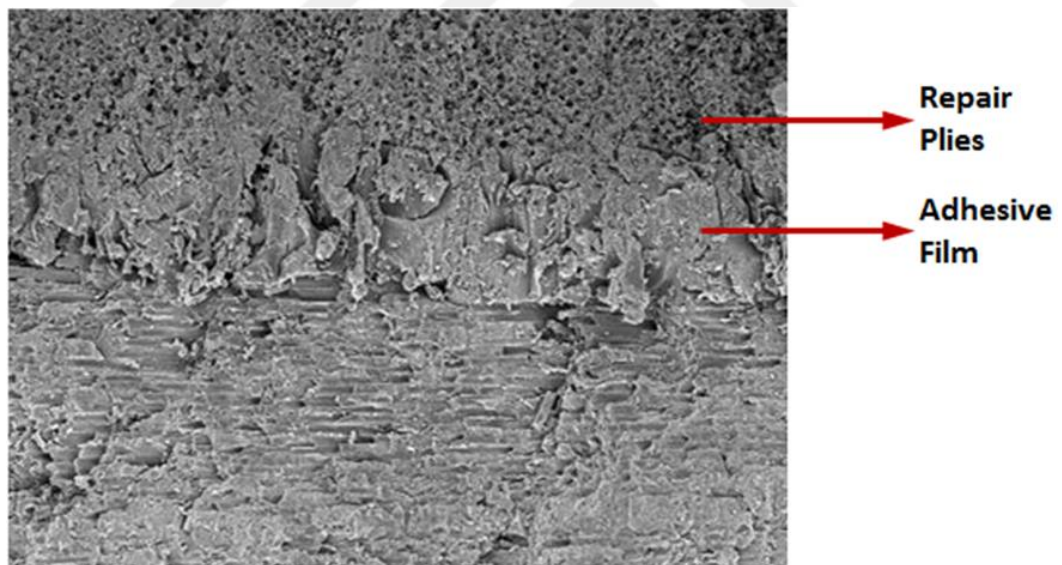


Figure 6.7: The SEM view 1.2 for the 0°-90° test specimens.

It was observed that the repair plies bonded perfectly with the original plies. No disbonding or delamination was observed during the SEM examinations. As expected, the repair plies had the same angularity as the plies removed for repair.

6.1.2 The Tensile Test Results for the 15° Test Specimens

Four pieces from the 10 test specimens were chosen to show in the stress/strain graph. The results given in Figure 6.8. are the ones closest to average.

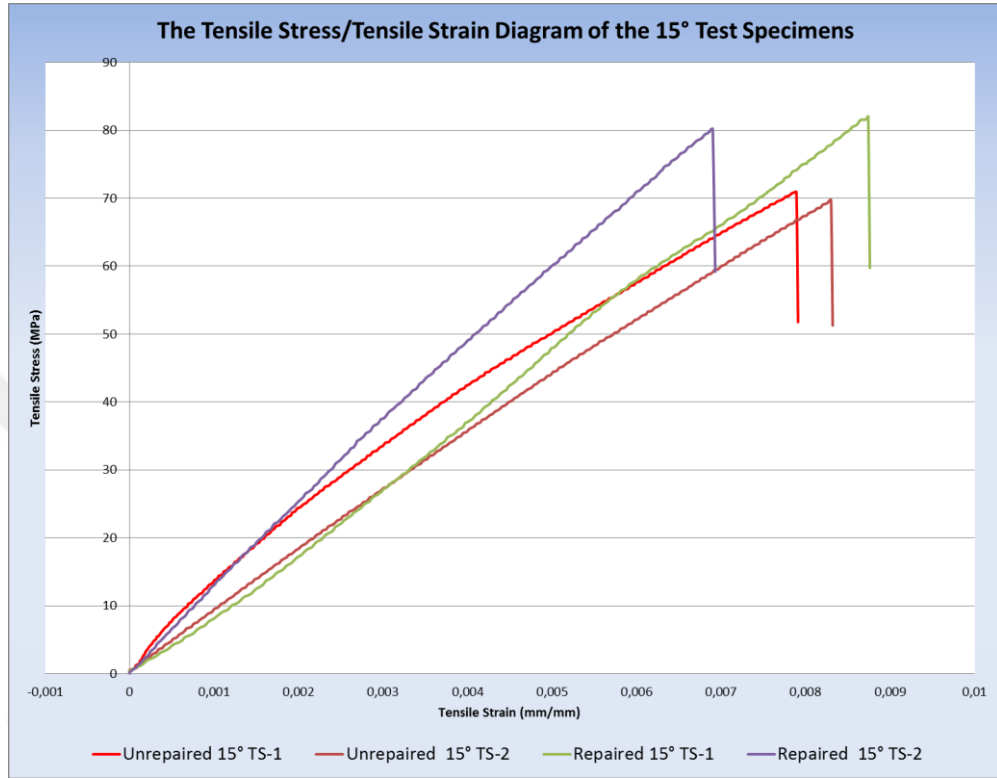


Figure 6.8: Four pieces from the 15° test specimens in the tensile stress/tensile strain graph.

Table 6.2: The tensile test results of the 15° test specimens.

	Maximum Tensile Stress [MPa]		Maximum Tensile Stress [MPa]
Repaired TS-1(15°)	85	Unrepaired TS-1(15°)	73
Repaired TS-2(15°)	84	Unrepaired TS-2(15°)	73
Repaired TS-3(15°)	81	Unrepaired TS-3(15°)	71
Repaired TS-4(15°)	80	Unrepaired TS-4(15°)	70
Repaired TS-5(15°)	84	Unrepaired TS-5(15°)	70

It was observed that both the repaired and unrepaired 15° test specimens showed brittle properties in the stress/strain diagram (Figure 6.8). The “brittle” manner was due to the fact that the curve is linear until it breaks or fractures with no bending of the curve at high loads. Consequently, there is no permanent change in the original shape during this test and hence, no ductility.

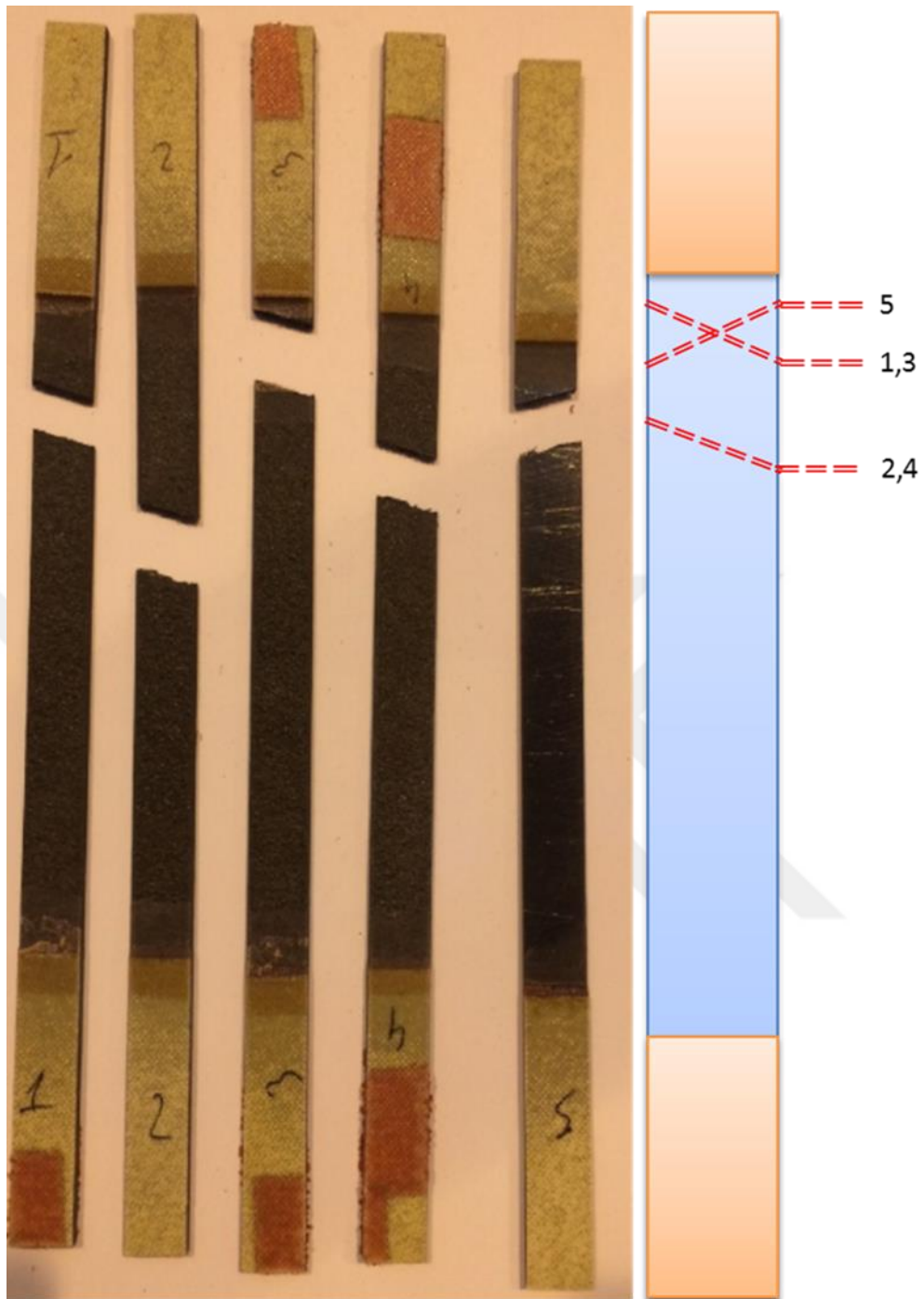


Figure 6.9: The unrepaired 15° test specimens after the tensile test.

The maximum tensile stresses of the unrepaired 15° test specimens were measured between 70 MPa and 73 MPa (Table 6.2).

The breakage points have the same angle as the original orientations (Figure 6.11).

As we examined the repaired test specimens at the same angle, the maximum tensile stresses on the unrepaired 15° test specimens were very low.

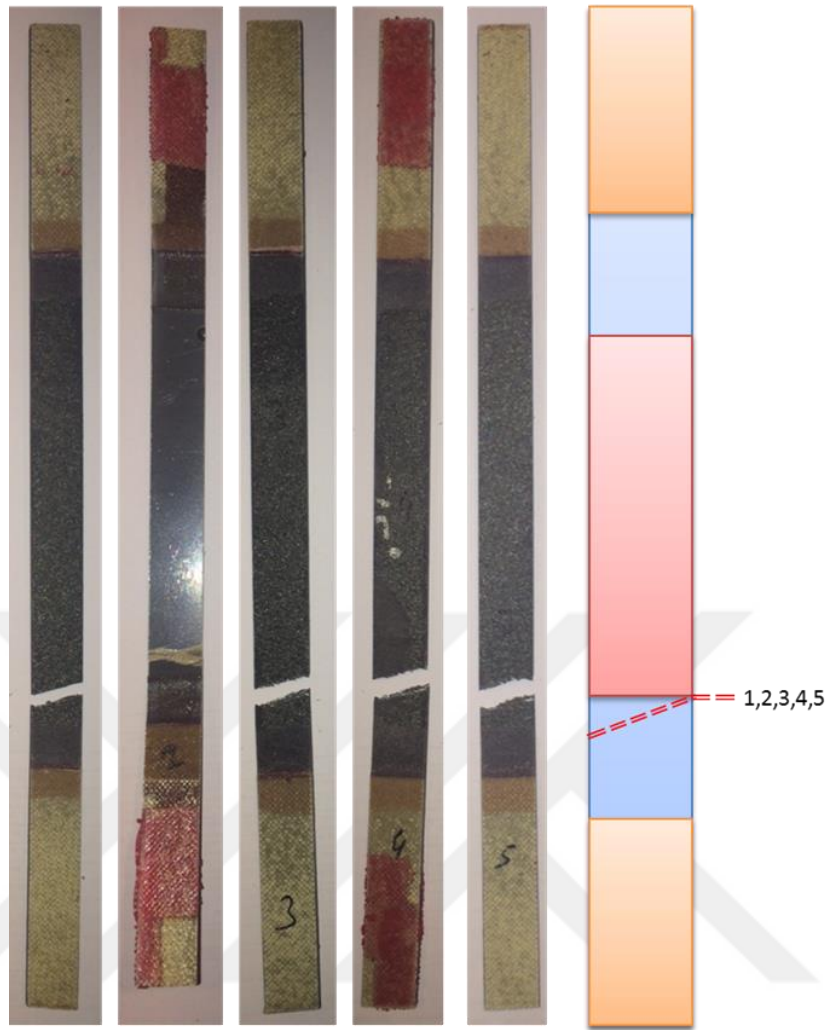


Figure 6.10: The repaired 15° test specimens after the tensile test.

It was observed that the repaired 15° lay-up test specimens had broken at approximately the same point. The breakage points start from the edges of the repair plies and continue for approximately 15° (Figure 6.11).

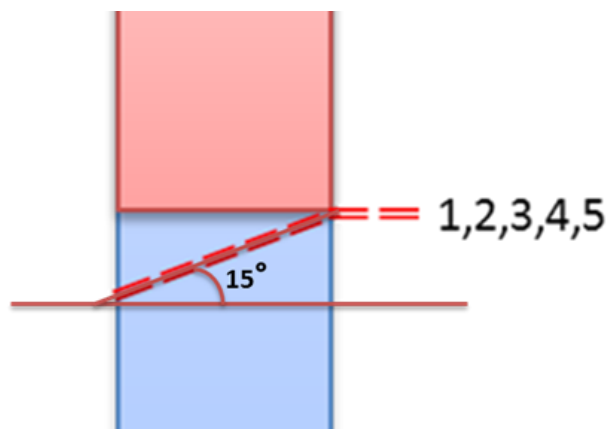


Figure 6.11: The breakage angle on the 15° test specimens after the tensile test.

The repair surface edges were observed to be the weakest points on the repaired 15° test specimens. The maximum tensile stresses of the repaired 15° test specimens were measured between 80 MPa and 85 MPa (Table 6.2).

The SEM examinations for the 15° test specimens:

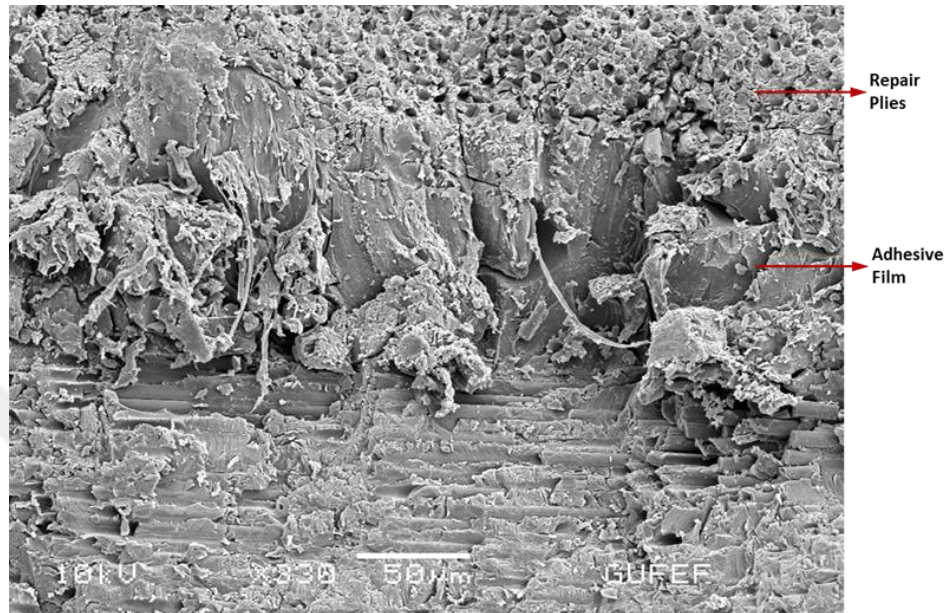


Figure 6.12: The SEM micrograph 2.1 for the 15° test specimens.

A very small disbonding was observed on the original plies. The waterjet cut method which was used to cut the SEM test specimens may cause this discrepancy in disbonding.

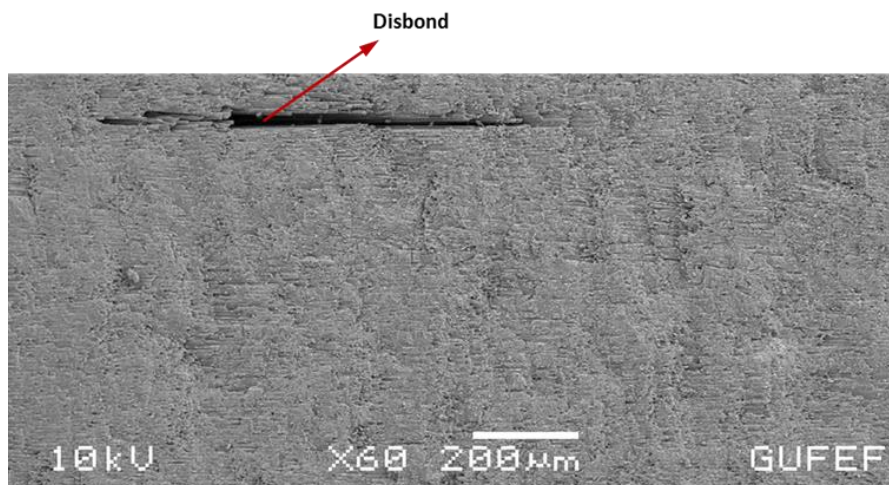


Figure 6.13: The SEM micrograph 2.2 for the 15° test specimens.

It was observed that the repair plies bonded perfectly to the original plies. As expected, the repair plies had the same angularity as the plies removed for repair.

6.1.3 The Tensile Test Results for the 30° Test Specimens

Four pieces from the 10 test specimens were chosen to show in the stress/strain graph (Figure 6.14). The results are the ones closest to average.

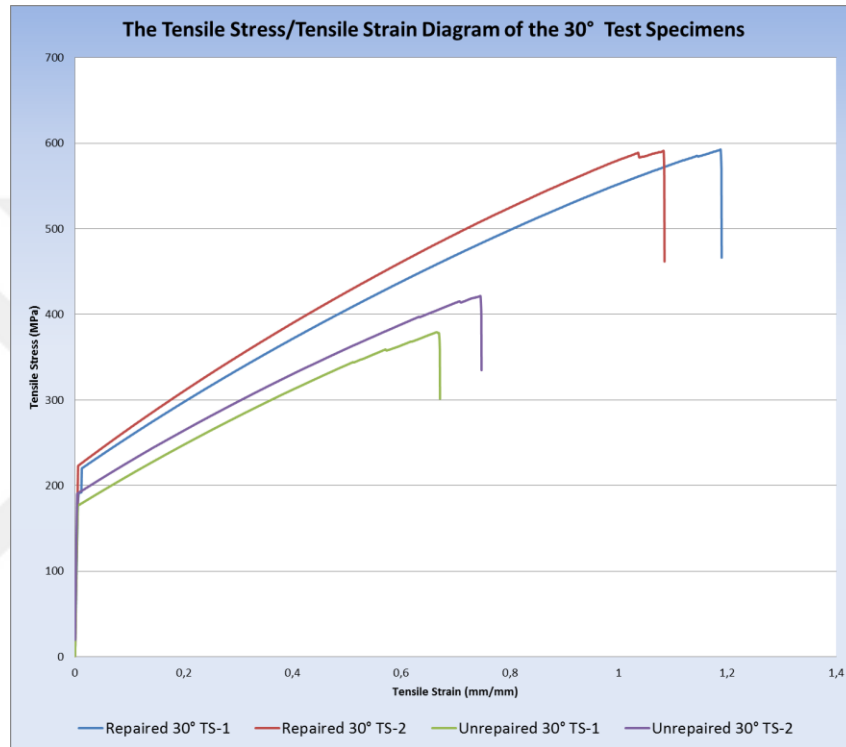


Figure 6.14: Four pieces from the 30° test specimens in the tensile stress/tensile strain graph.

Table 6.3: The tensile test results of the 30° test specimens.

	Maximum Tensile Stress [MPa]		Maximum Tensile Stress [MPa]
Repaired TS-1(30°)	589	Unrepaired TS-1(30°)	410
Repaired TS-2(30°)	587	Unrepaired TS-2(30°)	390
Repaired TS-3(30°)	598	Unrepaired TS-3(30°)	379
Repaired TS-4(30°)	919	Unrepaired TS-4(30°)	421
Repaired TS-5(30°)	731	Unrepaired TS-5(30°)	414

It was observed that 5 pieces of the unrepaired 30° test specimens had broken at approximately the same point (Figure 6.15). The maximum tensile stresses of the test specimens were measured between 379 MPa and 421 MPa (Table 6.3). When the

unrepaired 30° test specimens and repaired 30° test specimens were compared, it was found that the repaired materials had stronger tensile strength resistances.

It was observed that the yield points of the repaired 30° test specimens were higher than the unrepaired ones (Figure 6.14).

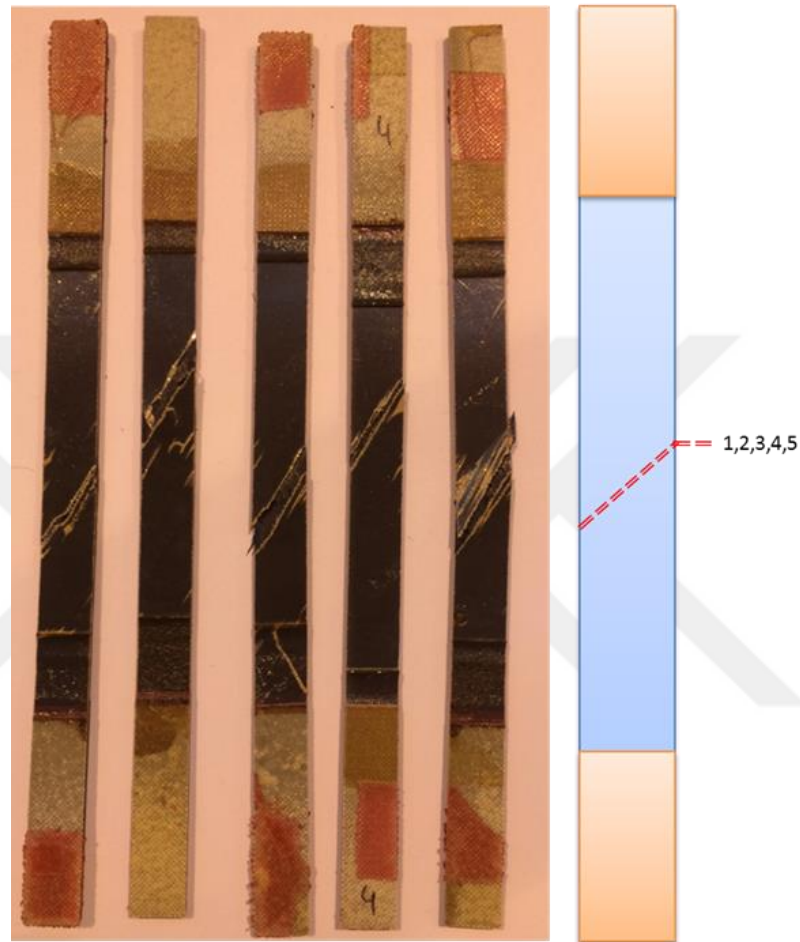


Figure 6.15: The unrepaired 30° test specimens after the tensile test

The tensile test showed that the repaired 30° test specimens had very high tensile stress resistances (Figures 6.34 and 6.35). The maximum tensile stresses of the 30° lay-up test specimens were measured between 587 MPa and 919 MPa (Table 6.3). As was shown in Figure 6.17., all of the repaired 30° test specimens fell to pieces during the tensile test. Breakages started from the edges of the largest repair plies, which are on the external surface (Figure 6.16).

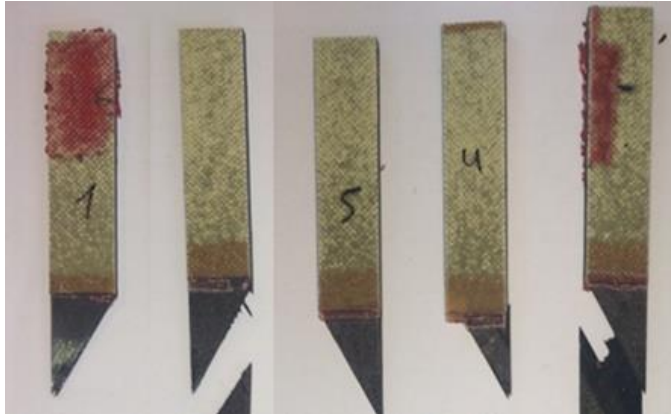


Figure 6.16: The breakage points of the repaired 30° test specimens.

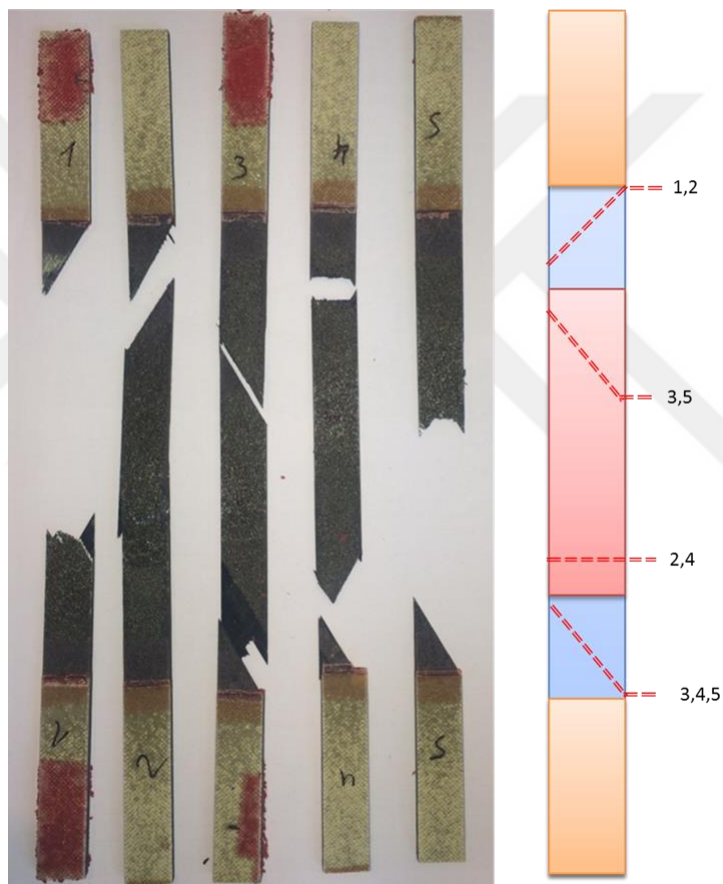


Figure 6.17: The repaired 30° test specimens after the tensile test.

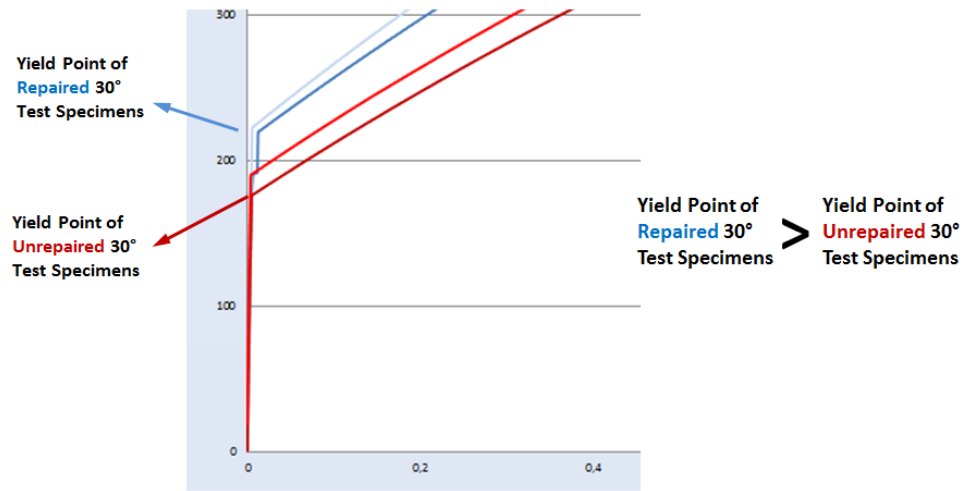


Figure 6.18: The yield strength points of the 30° test specimens.

We observed that repaired test specimens have higher yield strength points (Figure 6.18).

The SEM examinations for the 30° test specimens:



Figure 6.19: The SEM micrograph 3.1 for the 30° test specimens.

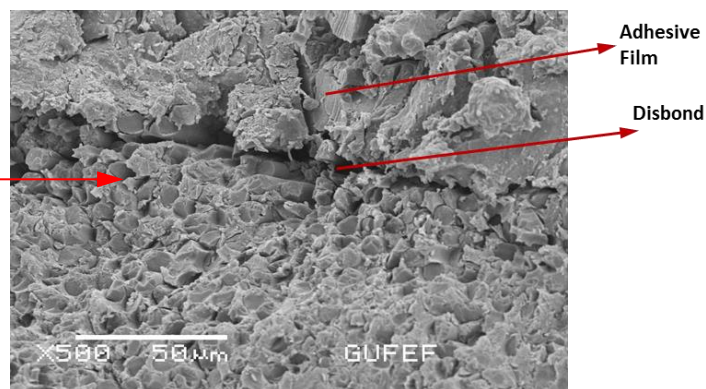


Figure 6.20: The SEM micrograph 3.2 for the 30° test specimens.

A disbonding discrepancy was observed between the repaired plies and the original plies, but this disbanding was at a tolerable level and the test specimens were acceptable in accordance with the related AIRBUS specifications. As can be observed in Figure 6.21. below, some more disbond micrographs were taken of the 30° test specimens, but they were all acceptable.

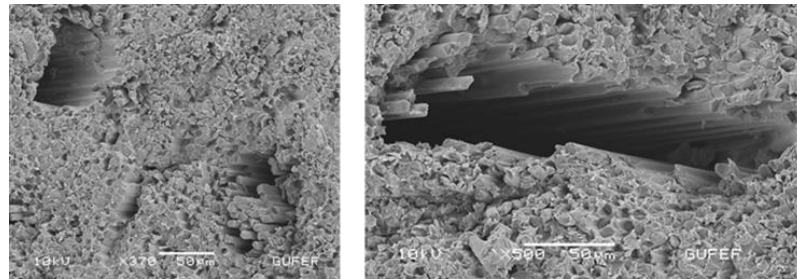


Figure 6.21: The SEM micrograph 3.3 for the 30° test specimens.

6.1.4 The Tensile Test Results for the 45° Test Specimens

Four pieces from the 10 test specimens were chosen to show in the stress/strain graph (Figure 6.22). The results are the ones closest to average.

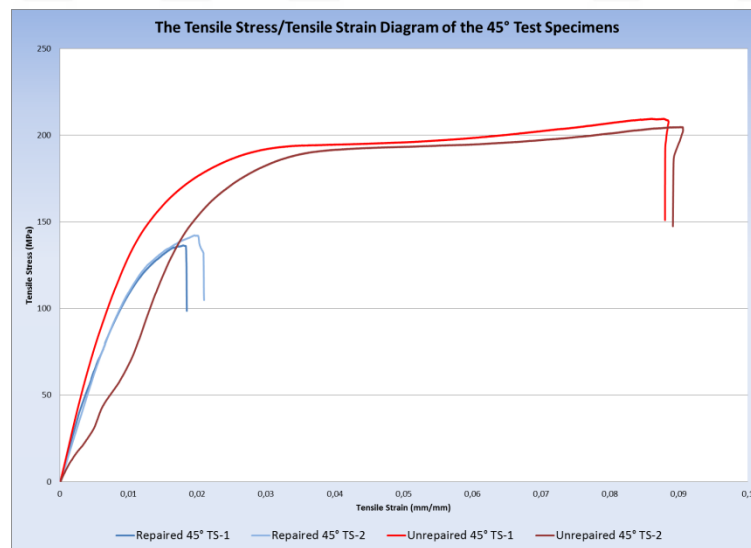


Figure 6.22: Four pieces from the 45° test specimens in the tensile stress/tensile strain graph.

Table 6.4: The tensile test results of the 45° test specimens.

	Maximum Tensile Stress [MPa]		Maximum Tensile Stress [MPa]
Repaired TS-1(45°)	133	Unrepaired TS-1(45°)	210
Repaired TS-2(45°)	142	Unrepaired TS-2(45°)	201
Repaired TS-3(45°)	144	Unrepaired TS-3(45°)	205
Repaired TS-4(45°)	136	Unrepaired TS-4(45°)	191
Repaired TS-5(45°)	138	Unrepaired TS-5(45°)	197

It was observed that 5 pieces of the unrepaired 45° test specimens had broken at approximately the same point (Figure 6.23). The maximum tensile stresses of the unrepaired 45° test specimens were measured between 191 MPa and 210 MPa (Table 6.4). As can be observed in Figure 6.24., the repaired 45° test specimens were broken from the middle of the test specimens. The maximum tensile stresses of the 45° test specimens were measured between 133 MPa and 144 MPa (Table 6.4).

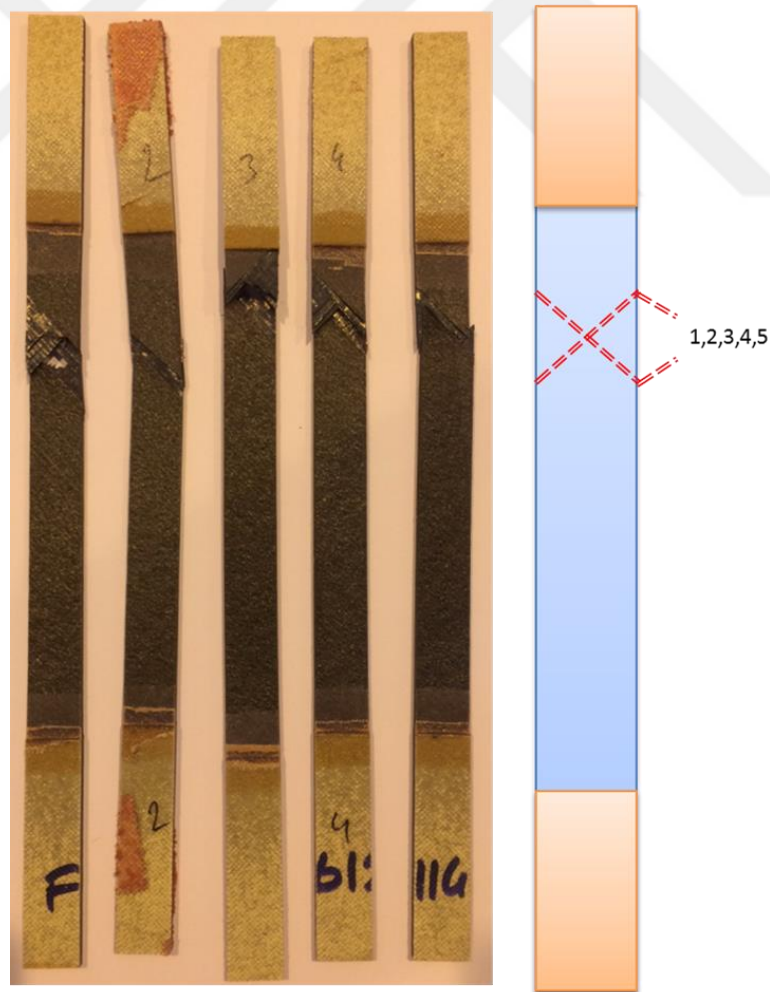


Figure 6.23: The unrepaired 45° test specimens after the tensile test.

As can be observed in Figure 6.23, the breakage angles are the same as the lay-up orientations.

The breakages were starting from the repair plies (Figure 6.23) on the repaired test specimen materials, but were broken close to the mid-point on the unrepaired/original test specimens (Figure 6.24).

Repair plies can be seen on Figure 6.25. We observed that breakages started from the smallest repair ply.

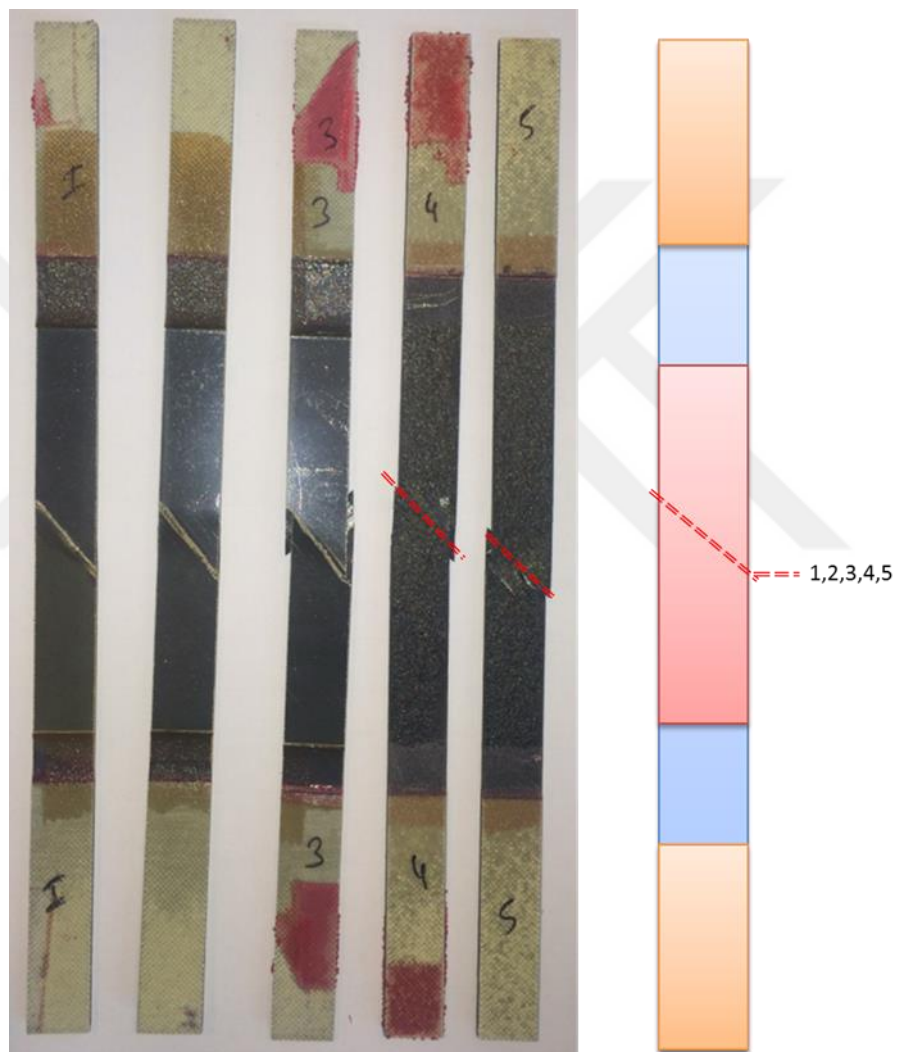


Figure 6.24: The repaired 45° test specimens after the tensile test.

The breakage/crack starting point has been shown in Figure 6.25

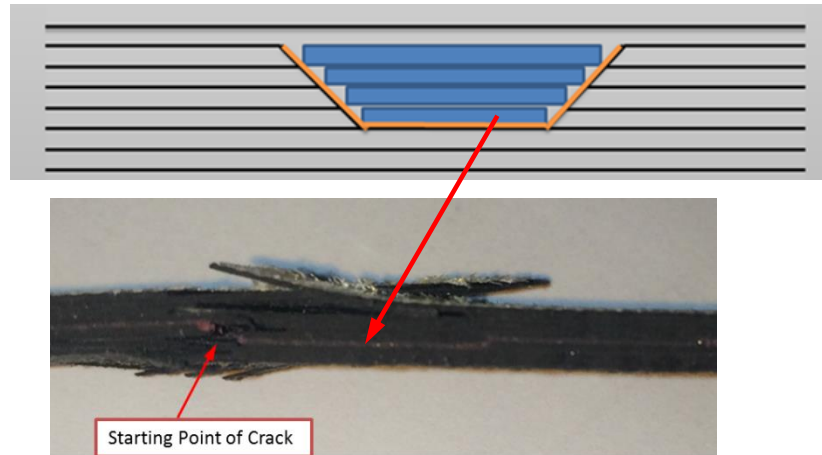


Figure 6.25: The repaired 45° test specimens after the tensile test.

The SEM examinations for the 45° test specimens:

We examined that the repair plies bonded perfectly to the original plies and there were no disbanding discrepancy.

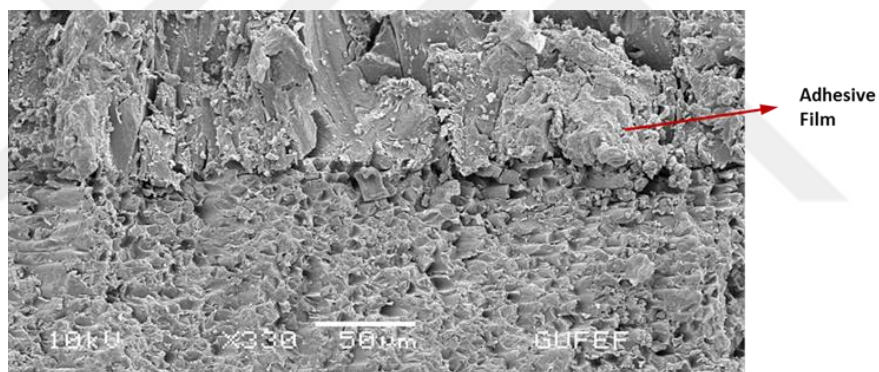


Figure 6.26: The SEM micrograph 4.1 for the 45° test specimens.

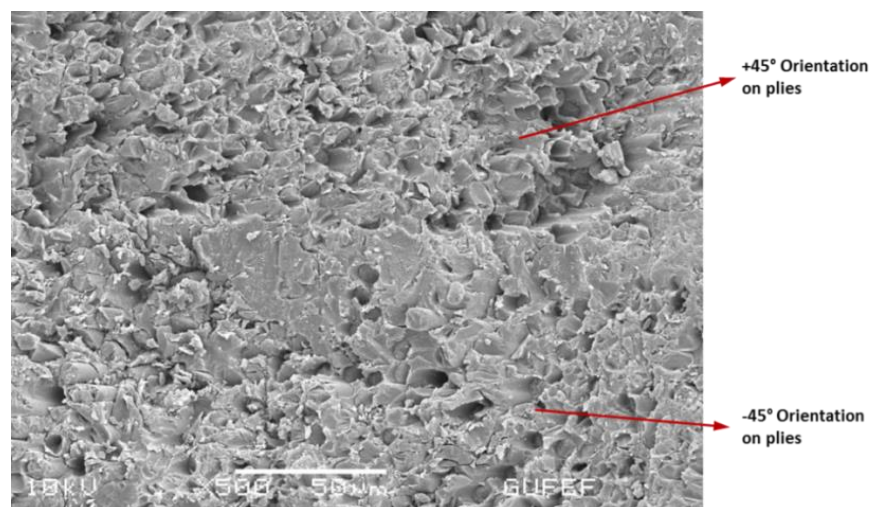


Figure 6.27: The SEM micrograph 4.2 for the 45° test specimens.

The ply orientation has been shown in Figures 6.27. and 6.28.

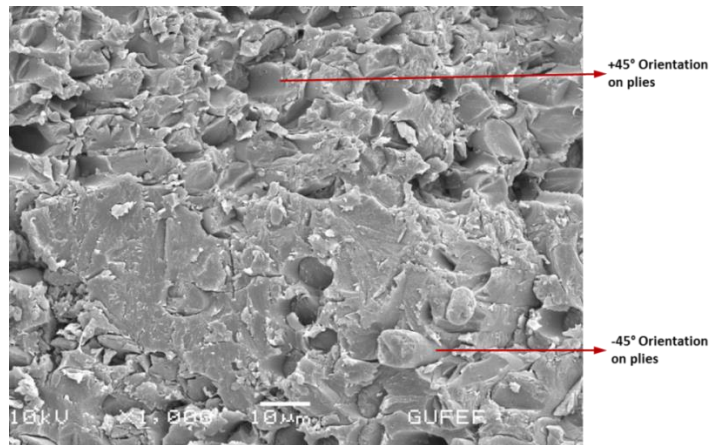


Figure 6.28. The SEM micrograph 4.3 for the 45° test specimens.

6.1.5 The Tensile Test Results for the 60° Test Specimens

Four pieces from the 10 test specimens were chosen to show in the stress/strain graph (Figure 6.29). The results are the ones closest to average.

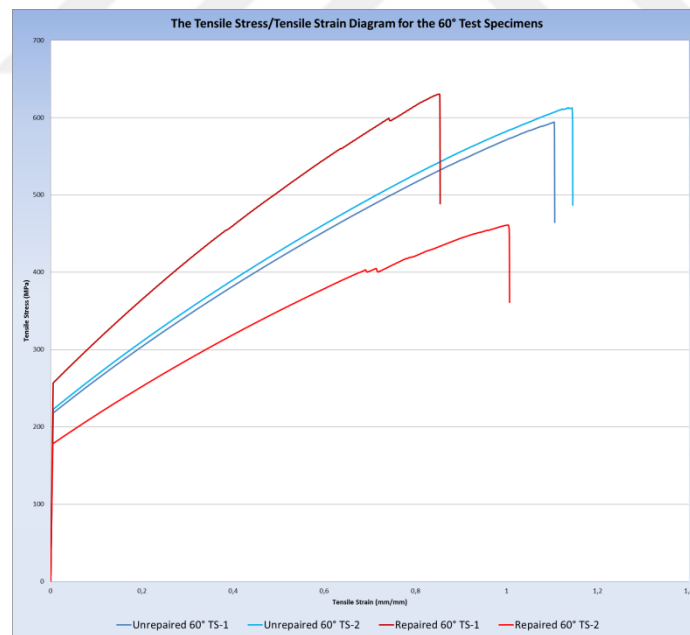


Figure 6.29: Four pieces from the 60° test specimens in the tensile stress/tensile strain graph.

Table 6.5: The tensile test results of the 60° test specimens.

	Maximum Tensile Stress [MPa]		Maximum Tensile Stress [MPa]
Repaired TS-1(60°)	632	Unrepaired TS-1(60°)	613
Repaired TS-2(60°)	692	Unrepaired TS-2(60°)	594
Repaired TS-3(60°)	491	Unrepaired TS-3(60°)	593
Repaired TS-4(60°)	557	Unrepaired TS-4(60°)	591
Repaired TS-5(60°)	548	Unrepaired TS-5(60°)	604

It was observed that 5 pieces of the unrepaired 60° test specimens had broken from approximately the same point. There were 2 breakage points on all of the test specimens (Figure 6.30). The maximum tensile stresses of the test specimens were measured between 591 MPa and 613 MPa (Table 6.5). Breakage points were very close and cracks had the same angles as the original orientations.

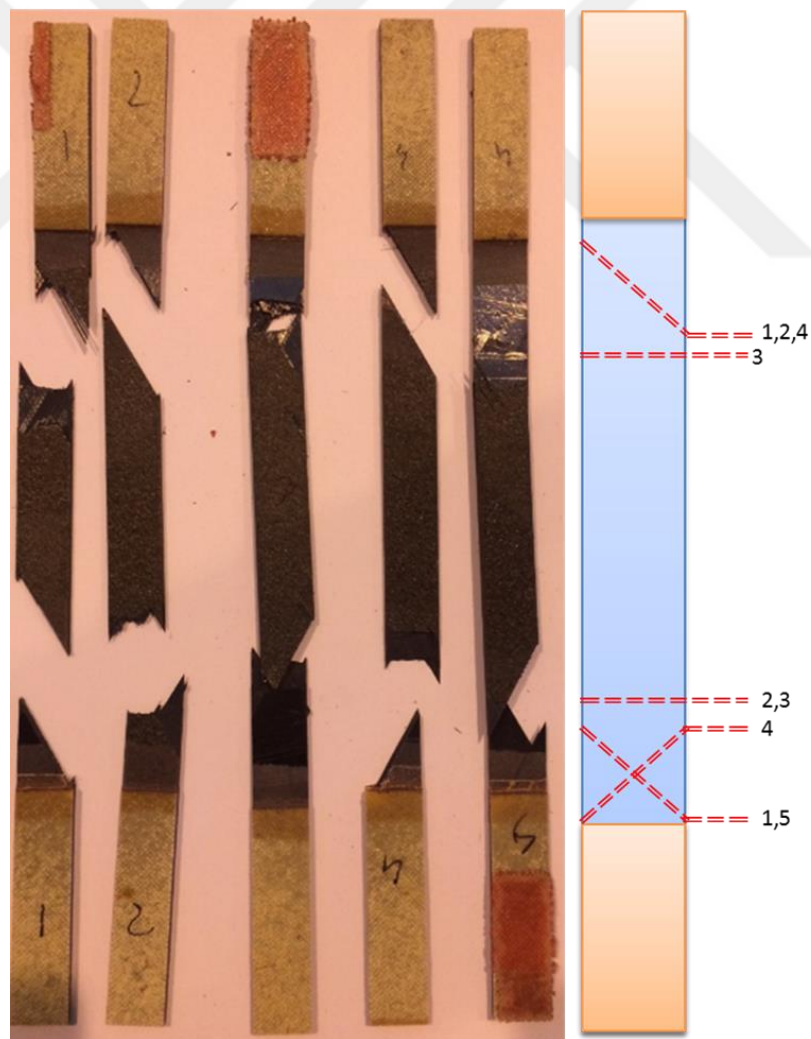


Figure 6.30: The unrepaired 60° test specimens after the tensile test.

As shown in Figure 6.31., all of the repaired 60° test specimens fell to pieces during the tensile test. The repaired 60° test specimens had high tensile stress resistances, like the repaired 30° lay-up test specimens (Table 6.4). The maximum tensile stresses of the repaired 60° test specimens were measured between 491 MPa and 692 MPa. Breakages started at the edges of the largest repair plies, which are on the external surface.

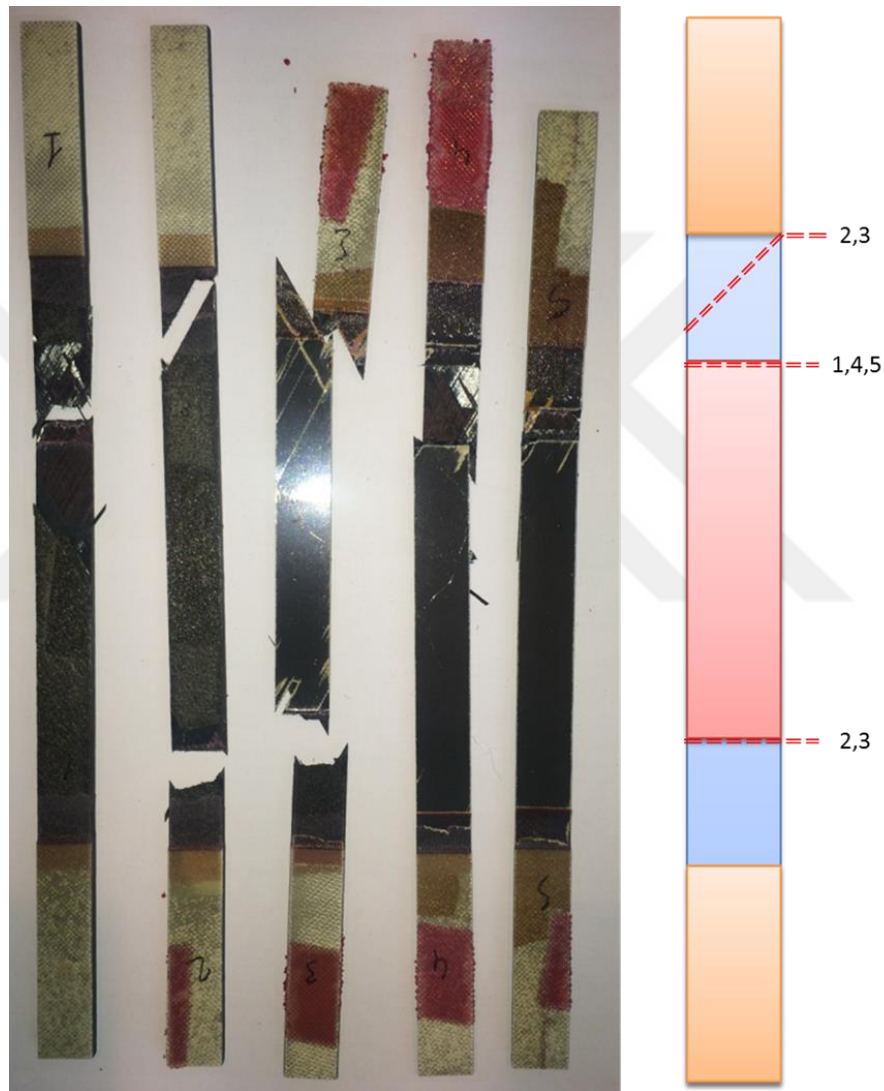


Figure 6.31: The repaired 60° test specimens after the tensile test.

When both the unrepaired and repaired test specimens that were examined were compared, it was found that the breakage points and maximum tensile stresses were very close and very high.

Approximately all of the breakages were starting close to the end tabs. The unrepaired 60° test specimens had high tensile stress resistances, like the repaired

60° lay-up test specimens. Cracks were more similar in the repaired 30° lay-up test specimens (Figures 6.17 and 6.31).

The SEM examinations for the 60° test specimens:

Different ply orientations were observed on Figure 6.32. and 6.33. And also we examined that the repair plies bonded perfectly to the original plies and there were no disbanding discrepancy.

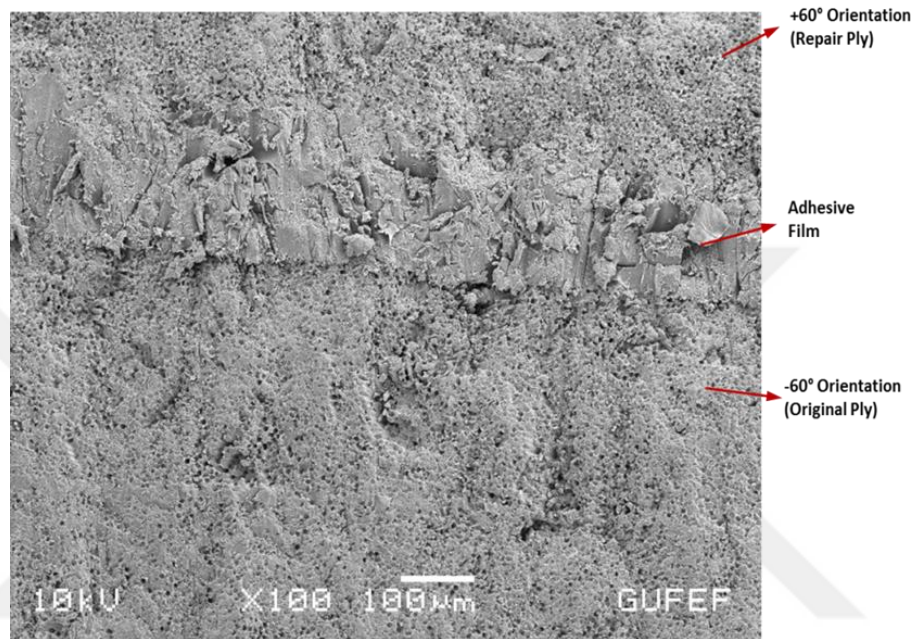


Figure 6.32: The SEM micrograph 4.1 for the 60° test specimens.

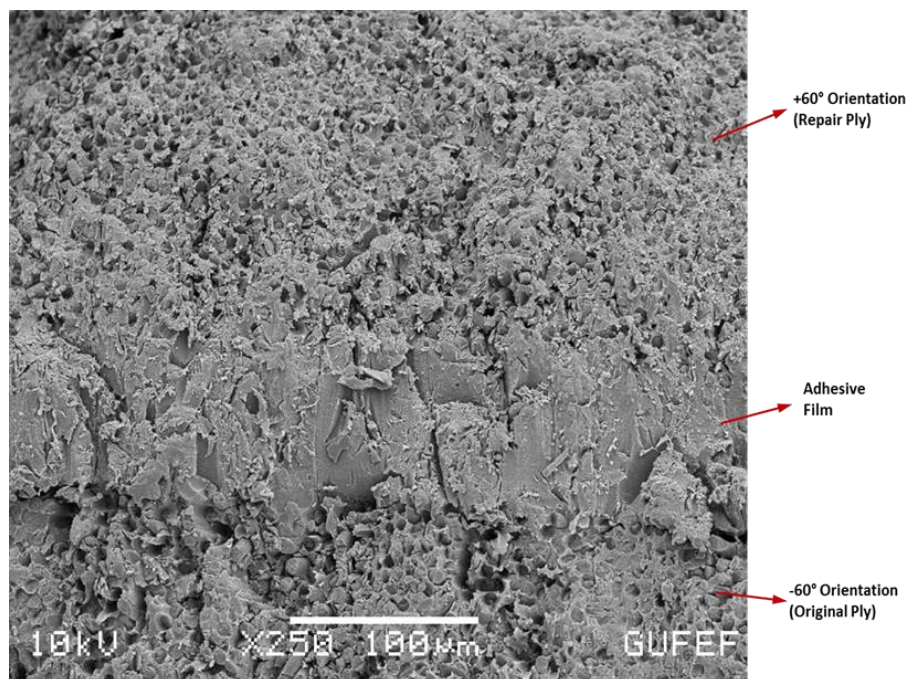


Figure 6.33: The SEM micrograph 4.2 for the 60° test specimens.

6.2 Summary of Chapter

The maximum tensile stresses of the unrepaired test specimens were measured between 70 MPa to 912 MPa (Table 6.6). The unrepaired 0°-90° test specimens had the highest tensile stress resistances. The unrepaired 15° test specimens had the weakest tensile stress resistances. The maximum tensile stresses for all of the unrepaired test specimens have been shown in Table 6.6. for an easy comparison of all of them together.

The results of the unrepaired test specimens did not have closer values, like the repair test specimens. Closer values were found for the test results of the 60° test specimens and the 30° test specimens. The largest difference examined was for the unrepaired 0°-90° test specimens that had the highest tensile stress resistances.

Table 6.6: The tensile test results of the unrepaired test specimens.

Specimen Title	Maximum Tensile Stress [MPa]
Unrepaired TS-4(15°)	70
Unrepaired TS-5(15°)	70
Unrepaired TS-3(15°)	71
Unrepaired TS-1(15°)	73
Unrepaired TS-2(15°)	73
Unrepaired TS-4(45°)	191
Unrepaired TS-5(45°)	197
Unrepaired TS-2(45°)	201
Unrepaired TS-3(45°)	205
Unrepaired TS-1(45°)	210
Unrepaired TS-3(30°)	379
Unrepaired TS-2(30°)	390
Unrepaired TS-1(30°)	410
Unrepaired TS-5(30°)	414
Unrepaired TS-4(30°)	421
Unrepaired TS-4(60°)	591
Unrepaired TS-3(60°)	593
Unrepaired TS-2(60°)	594
Unrepaired TS-5(60°)	604
Unrepaired TS-1(60°)	613
Unrepaired TS-2(0°-90°)	880
Unrepaired TS-1(0°-90°)	887
Unrepaired TS-3(0°-90°)	902
Unrepaired TS-4(0°-90°)	904
Unrepaired TS-5(0°-90°)	912

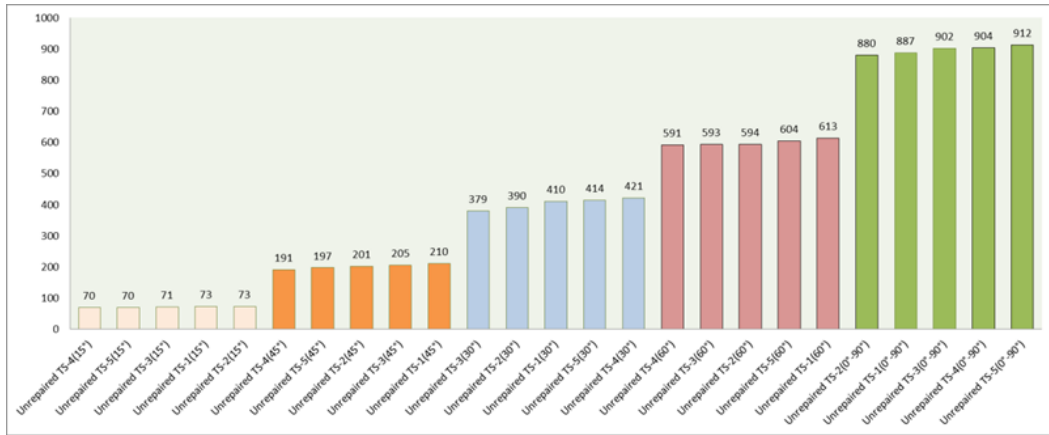


Figure 6.34: The maximum tensile stress resistances for all of the unrepaired test specimens compared in the same graph.

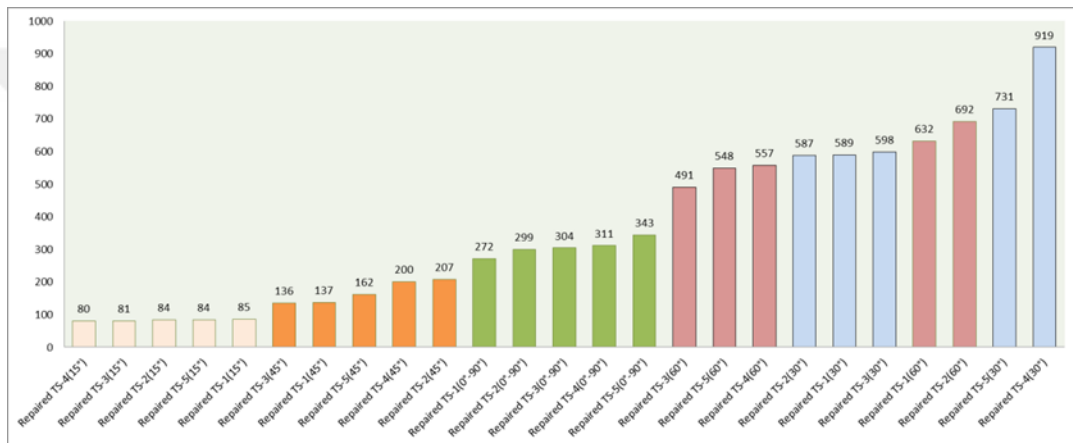


Figure 6.35: The maximum tensile stress resistances for all of the repaired test specimens compared in the same graph.

The ultimate tensile stress points of the repaired test specimens were measured between 80 MPa to 919 MPa (Table 6.7).

The repaired 30° test specimens had the highest tensile stress resistances. The repaired 15° test specimens had the weakest tensile stress resistances. The maximum tensile stresses for all of the repaired test specimens have been shown in Table 6.7. for an easy comparison of all of them together. Most of the breakages were starting at the edges of the repair plies. The results of the repaired 60° test specimens and the repaired 30° test specimens had closer values than the other ply orientations.

Table 6.7: The tensile test results of the repaired test specimens.

Specimen Title	Maximum Tensile Stress [MPa]
Repaired TS-4(15°)	80
Repaired TS-3(15°)	81
Repaired TS-2(15°)	84
Repaired TS-5(15°)	84
Repaired TS-1(15°)	85
Repaired TS-3(45°)	133
Repaired TS-1(45°)	142
Repaired TS-5(45°)	144
Repaired TS-4(45°)	136
Repaired TS-2(45°)	138
Repaired TS-1(0°-90°)	272
Repaired TS-2(0°-90°)	299
Repaired TS-3(0°-90°)	304
Repaired TS-4(0°-90°)	311
Repaired TS-5(0°-90°)	343
Repaired TS-3(60°)	491
Repaired TS-5(60°)	548
Repaired TS-4(60°)	557
Repaired TS-2(30°)	587
Repaired TS-1(30°)	589
Repaired TS-3(30°)	598
Repaired TS-1(60°)	632
Repaired TS-2(60°)	692
Repaired TS-5(30°)	731
Repaired TS-4(30°)	919

Two pieces from all of the lay-up orientations were chosen for being able to make a better comparison and analysis of the tensile stress/strain for the unrepaired test specimens in the same diagram. All of the relevant comments have been given in the conclusions.

The variation of tensile strength for different orientations is significant in unrepaired composites compared to their repaired counter partners.

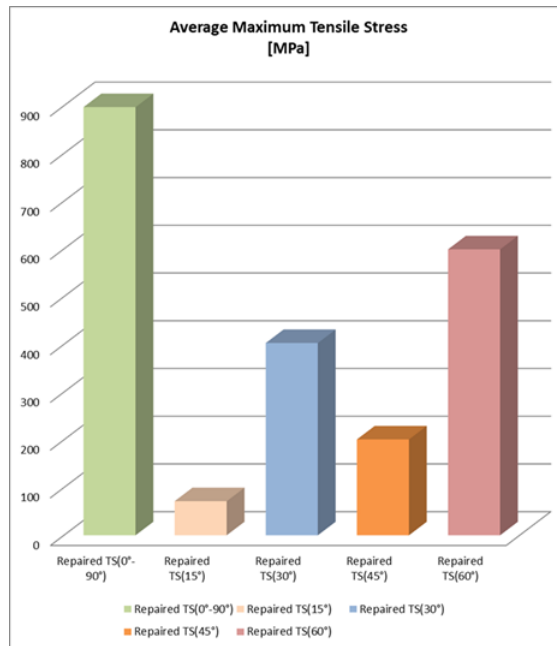


Figure 6.36: Average ultimate strength points of the unrepaired test specimens.

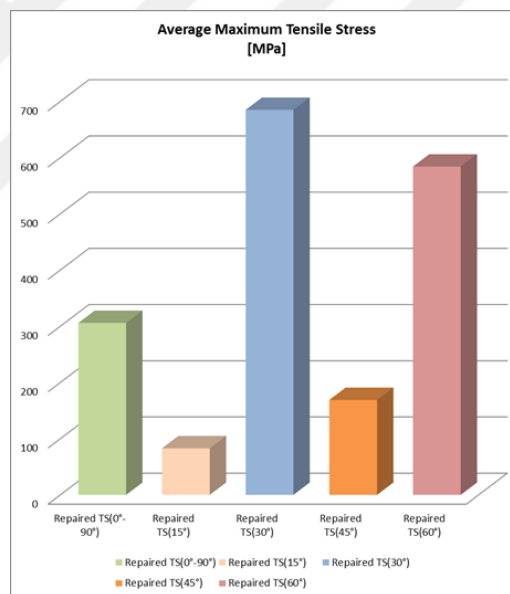


Figure 6.37: Average ultimate strength points of the repaired test specimens.

The tensile test was applied to examine the mechanical properties of the test specimens. The average results have been given in Figures 6.36., 6.37. and Table 7.1.

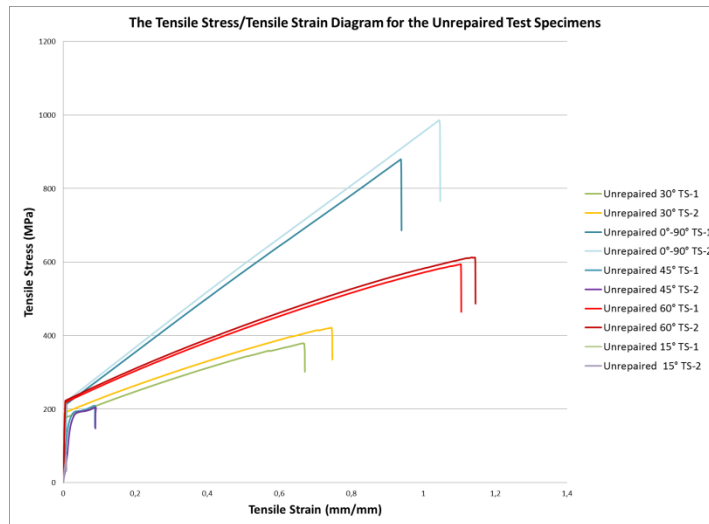


Figure 6.38: The tensile stress/tensile strain diagram for the unrepaired test specimens.

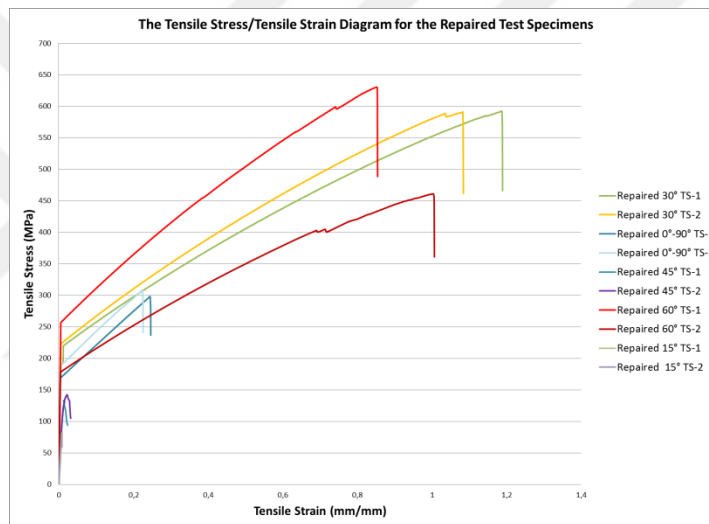


Figure 6.39: The tensile stress/tensile strain diagram for the repaired test specimens.

Figures 6.38 and Figure 6.39 and Table 7.2 presents the yield point of repaired and unrepaired specimens. It was observed that yield strengths are relatively closer to each other for both type of specimen in contrast to some significant deviation in their post-elastic response such as average ultimate strength points.

CHAPTER SEVEN

CONCLUSIONS

The repaired and unrepaired carbon fiber composite materials have been examined and compared in this thesis. The test specimens were composed of 12 plies and the preferred orientations of the plies was 0° - 90° , 15° , 30° , 45° and 60° .

According to the results of the tensile test, the unrepaired 0° - 90° test specimens had the highest values. It was observed that the unrepaired and repaired results of the 15° , 45° and 60° test specimens had proximate values on the same angles. The results showed that only for 30° test specimens, the repaired test specimens had higher ultimate strength values compared to unrepaired ones (Table 7.1). We here conclude that repair of the composite materials with 30° ply angle enhance their mechanical performance, while an opposite effect was observed for those of 0° - 90° .

Table 7.1: Average ultimate strength points for all of the test specimens.

Unrepaired 0° - 90° (897 Mpa)	>	Repaired 0° - 90° (305,8 Mpa)
Repaired 15° (82,8 Mpa)	>	Unrepaired 15° (71,4 Mpa)
Repaired 30° (684,8 Mpa)	>	Unrepaired 30° (402,8 Mpa)
Unrepaired 45° (200,8 Mpa)	>	Repaired 45° (138,6 Mpa)
Unrepaired 60° (599 Mpa)	>	Repaired 60° (584 Mpa)

When the breakage points were analyzed, most of the breakages started from the repair plies on the repaired parts. The main comment on this situation is that the repair plies are the weakest points on the repaired parts. However, if the general results are checked for all of the test specimens, then it can be said that repairs may sometimes could obtain stronger tensile resistances compared to the original test specimens such as ply angle of 30° .

Our experimental work experience in this study shed light on the fact that to improve the repair performances, different lay-up angles on the repair plies, different curing methods and different cure temperatures can be examined in the future.

Table 7.2: Average yield strength points for all of the test specimens.

	Average of Yield Strength Points
Repaired 0°-90°	179,5
Repaired 15°	Brittle
Repaired 30°	208
Repaired 45°	Brittle
Repaired 60°	218
Unrepaired 0°-90°	216,5
Unrepaired 15°	Brittle
Unrepaired 30°	182,5
Unrepaired 45°	191,5
Unrepaired 60°	222

As it is known, the disbonding discrepancies were not only on the different angles of the plies that were examined in the SEM micrographs, but there can also be a disbonding discrepancy inside the same ply. The disbonding discrepancies discovered in the SEM micrographs were determined to be too small to be detected. In addition, all of the disbondings discovered were measured and evaluated to be within the acceptable limits according to the specifications.

7.1 Recommended Future Research

In the future, numerical tensile modelling of the composite material for both unrepaired and repaired types of different ply angles were developed to get an insight about the underlying physics of the experimental work discussed in this thesis.

REFERENCES

- 1) <https://compositesuk.co.uk/compositematerials>
- 2) Wikipedia, https://en.m.wikipedia.org/wiki/Composite_repairs
- 3) Wikipedia, https://en.m.wikipedia.org/wiki/Composite_material
- 4) F.C. Campbell (2010). Structural Composite Materials. Chapter 1
- 5) www.efunda.com Introduction to Composite Materials
- 6) A.A. Baker, L.R.F. Rose, Rhys Jones. Advances in the Bonded Composite Repair of Metallic Aircraft Structure, Volume 1
- 7) Pichai Rusmee (1998-2005). High Strength Composites
- 8) K. Kawamura, M. Ono, and K. Okazaki, Carbon 30(3), 429-434 (1992).
- 9) Deborah D. L. Chung. Carbon Fiber Composites. Chapter 1. (1994)
- 10) Autar K. Kaw. Mechanics Of Composite Materials, 2nd edition (2006).
- 11) FAA. Advanced Composite Materials, Chapter 7. (2012)
- 12) T.D. Breitzman, E.V. Iarve, B.M. Cook, G.A. Schoeppner, R.P. Lipton, Optimization of a composite scarf repair patch under tensile loading (2009)
- 13) Wang, C.H. and Gunnion, A.J., Optimum Shapes for Minimising Bond Stress in Scarf Repairs. Proc. 5th Australasian Congress on Applied Mechanics (ACAM 2007), Brisbane, Australia, (717-722). 10-12 December, 2007.
- 14) Baker, A.A., A Proposed Approach for Certification of Bonded Composite Repairs to Flight-Critical Airframe Structure, Applied Composite Materials

- 15) Whittingham, B., Baker, A.A., Harman, A. and Bitton, D., Micrographic studies on adhesively bonded scarf repairs to thick composite aircraft structure, Composites: Part A 40 (2009)
- 16) Baker, A.A., Development of a Hard-Patch Approach for Scarf Repair of Composite Structure, DSTOTR-1892, 2006.
- 17) 9. Rider, A.N., Wang, C.H. and Chang, P., (2010) Bonded repairs for carbon/BMI composite at high operating temperatures, Composites: Part A 41 902–912
- 18) Net Composites, <http://www.netcomposites.com/>
- 19) Hart-Smith LJ. Adhesive-bonded scarf and stepped-lap joints. NASA;1973.
- 20) Advanced composite design guide. AFML Wright-Patterson air force base. Analysis, Vol. II. United States Air Force; 1973.
- 21) Gunnion, A.J. and Herszberg, I., Parametric study of scarf joints in composite structures, Composite Structures, Volume 75, Issues 1-4, September 2006
- 22) Carbon fibre reinforced epoxy prepreg unidirectional tape 180°C – curing class standard modulus fiber structural material
- 23) AIRBUS IPS10-01-003-01
- 24) Cartz, Louis (1995). Nondestructive Testing. A S M International.
- 25) <http://www.ndted.org/EducationResources/CommunityCollege/PenetrantTest/Introduction/history.htm>
- 26) ASTM E1316: "Standard Terminology for Nondestructive Examinations", The American Society for Testing and Materials, in Volume 03.03 NDT, 1997
- 27) Dufour, M. L.; Lamouche, G.; Detalle, V.; Gauthier, B.; Sammut, P. (April 2005). "Low Coherence Interferometry, an Advanced Technique for Optical Metrology in Industry". Insight Non Destructive Testing and Condition Monitoring 47 (4): 216–219.
- 28) Czichos, Horst (2006). Springer Handbook of Materials Measurement Methods. Berlin: Springer. P. 303–304.

- 29) Davis, Joseph R. (2004). Tensile testing (2nd ed.). ASM International.
- 30) W.F. Hosford (1992). Overview of Tensile Testing, Tensile Testing, P. Han, Ed., ASM International, P 1–24
- 31) Standard test method for tensile properties of polymer matrix composite materials: ASTM D3039
- 32) European Standard DNA-EN-2563 (1997)
- 33) Harman, A.B., and Wang, C.H., Improved design methods for scarf repairs to highly strained composite aircraft structure, Composite Structures 75 (2006)
- 34) Andrew J. Gunnion, Israel Herszberg, Parametric study of scarf joints in composite structures (2006)
- 35) MIL-HDBK-17-3F. Composite materials handbook: Supportability, vol. 3. Department of Defence [chapter 8].
- 36) Oplinger DW. Mechanical fastening and adhesive bonding. In: Peters ST, editor. Handbook of composites. London: Chapman & Hall; 1998. p. 610–66.
- 37) Hart-Smith LJ. Advances in the analysis and design of adhesive bonded joints in composite aerospace structures. In: SAMPE process engineering series, vol. 19. Asusa: SAMPE; 1974, p. 722–37.
- 38) Hart-Smith LJ. Adhesively bonded joints in fibrous composite structures. Douglas aircraft paper 7740. In: The international symposium on joining and repair of fibre-reinforced plastics, Imperial College, London; 1986.
- 39) Wang CH, Rider AN, Chang P, Charon A, Baker AA. Structural repair techniques for highly-loaded carbon/BMI composites. In: Proceedings of SAMPE fall technical conference, SAMPE Publishing; 2007. ISBN 978-1-934551-01-1.
- 40) Baker AA, Chester RJ, Hugo GR, Radtke TC. Scarf repairs to highly strained graphite/epoxy structure. Int J Adhes Adhes 1999;19:161–71.

RESUME

PERSONNEL INFORMATION

Name Surname : Fikret Cem SÖNMEZ
Place/Date of birth : Ankara/1984
E-mail : fcsonmez@tai.com.tr / fikretcemsonmez@gmail.com
Phone : +90 536 877 06 06

EDUCATION

High School : Ankara Ayrancı High School
University : Cumhuriyet University, Faculty of Engineering, Mechanical
Engineering

EXPERIENCE

2011 - Still Working : Turkish Aerospace Industries / Ankara, Quality Assurance
Engineer (Structural Assembly)

LANGUAGE

English